



Mohamed Khider University of Biskra
Faculty of exact sciences and natural and life sciences
Material sciences department

MASTER MEMORY

Domain of Matter Sciences
Section of Physics
Speciality Condensed Matter Physics
Réf. :

Prsented by:
Saada Khaoula

The:

Development and characterization of pure and doped ZnO nanopowder with Ga and Bi via the sol-gel method.

Jury:

| | | | | |
|-----|------------------|-----|----------------------|-----------|
| Mr. | Alakel Abdelghni | MCA | Université de Biskra | President |
| Mrs | Almi Kanza | MCA | Université de Biskra | Examiner |
| Ms | Arab Louiza | MCA | Université de Biskra | Reporter |

Academic Year: 2022-2023

بِسْمِ اللَّهِ الرَّحْمَنِ الرَّحِيمِ

DEDICATION

I dedicated this humble work to

My mother is my source of courage and inspiration, I devoted so much to seeing me get to this day.

To my father, the source of respect and appreciation.

May God Almighty save them for me and prolong me at their age.

To my dear sisters and brothers in his name Hamza, Maryam, Al khansa, Amina, Fatima...

To my friends Ines, Chams , Zahra, Ouissal, Siham...

To " Boudour Saif eddine" for his moral support.

To my teachers and teachers from primary school to university.

Everyone named here and all known.

ACKNOWLEDGEMENTS

First, we thank God Almighty, who has succeeded in completing this work despite some of the difficulties and obstacles we have faced.

After that, I thanked my family very much, especially my mother, the warrior woman who has always been and continues to support me in all my decisions.

*I also thank **Dr. Louiza Arab** and **Ms. Aya Latif** for their efforts and valuable advice throughout the work done.*

*We warmly thank the jury members: **Dr. Alakel Abdelghni** and **Dr. Almi Kenza** For agreeing to review our work.*

Finally, we offer our greetings to many people who, from near or far, have contributed to accomplished this work.

Table of Contents

| | |
|--|------|
| DEDICATION | I |
| ACKNOWLEDGEMENTS | II |
| List Of Figures | VI |
| List Of Tables | VIII |
| General Introduction | 1 |
| References | 3 |
| Chapter I Bibliographic studies | 4 |
| I.1. Zinc Oxide «ZnO» | 5 |
| I.2. Why choose ZnO specifically ? | 5 |
| I.3. Properties of zinc oxide..... | 6 |
| I.3.1. Physical Properties | 6 |
| I.3.1.1. Structural properties of ZnO | 7 |
| I.3.1.2. Electrical properties | 10 |
| I.3.1.3. Optical properties..... | 11 |
| I.3.1.4. Electronic band structure | 11 |
| I.3.1.5. Mechanical properties | 12 |
| I.3.2. Chemical Properties..... | 12 |
| I.3.3. Catalytic properties..... | 13 |
| I.4. ZnO doping | 13 |
| I.4.1. Doping with Bi | 14 |
| I.4.2. Doping with Ga | 14 |
| I.5. Nanomaterials | 15 |
| I.5.1. Nanoparticles | 15 |
| I.5.2. Classification of nanomaterials | 16 |
| I.6. Applications of zinc oxide | 17 |
| I.6.1. ZnO powder applications | 18 |
| I.6.2. ZnO applications in thin film | 18 |
| I.6.2.1. Solar Cells..... | 18 |
| I.6.2.2. Light emitting diodes | 19 |
| I.6.2.3. Gas sensor | 19 |
| I.6.2.4. Varistors..... | 20 |

| | |
|--|-----------|
| I.6.2.5. Medical | 20 |
| References | 21 |
| Chapter II methods and materials | 24 |
| II.1. Methods of synthesis of nanomaterials | 25 |
| II.2. The sol-gel method | 25 |
| II.2.1. Ways of the Sol-Gel process | 27 |
| II.2.1.1. Inorganic or colloidal route | 27 |
| II.2.1.2. Metallo-organic or polymeric pathway | 27 |
| II.2.2. Predominant chemical reactions..... | 28 |
| II.2.2.1. Hydrolysis reaction..... | 28 |
| II.2.2.2. Condensation reaction | 28 |
| II.2.3. The sol-gel transition..... | 29 |
| II.2.4. Study of gelification time | 30 |
| II.2.5. Drying | 30 |
| II.2.5.1. Xerogel | 30 |
| II.2.5.2. Aerogel | 31 |
| II.2.6. Parameters influencing the kinetics of reactions..... | 31 |
| II.2.7. Advantages and disadvantages of sol-gel | 32 |
| II.2.8. Applications of Sol Gel method | 32 |
| II.3. Preparation of pure ZnO powders doped with gallium «Ga» and «Bi» | 33 |
| II.3.1. Preparation Steps..... | 35 |
| II.3.1.1. Cleaning glass..... | 35 |
| II.3.1.2. Pure ZnO nano-powders | 35 |
| II.3.2.3. Bi-doped ZnO nano-powders | 36 |
| II.3.2.4. Ga+Bi co-doped ZnO nano-powders..... | 36 |
| II.3.3. Calcination treatment | 36 |
| II.4. ZnO powder characterization techniques | 39 |
| II.4.1. X-ray diffraction..... | 39 |
| II.4.1.1. Grain Size | 40 |
| II.4.1.2. The interreticular distances and the cell parameters..... | 40 |
| II.4.1.3. The lattice strain | 41 |
| II.4.1.4. The dislocation density | 41 |
| II.4.2. UV-Visible spectrophotometry | 41 |
| II.4.2.1. Absorption coefficient | 42 |
| II.4.2.2. Optical Gap E_g | 43 |

| | |
|---|-----------|
| II.4.2.3. Sample preparation | 43 |
| II.4.3. Fourier Transform Infrared Spectroscopy (FTIR) | 44 |
| II.4.3.1. Sample preparation | 45 |
| References | 47 |
| Chapter III Results and discussions | 50 |
| III.1 Results and discussions | 51 |
| III.1.1. structural study | 51 |
| III.1.1.1. Crystallite size, Lattice strain and Dislocation density variation | 53 |
| III.1.1.2. Lattice parameters | 55 |
| III.1.2. Optical study | 56 |
| III.1.3. Chemical study | 59 |
| References | 61 |
| General conclusion | 63 |
| Abstract | 65 |

List Of Figures

| | | |
|--------------|---|----|
| Figure I.1 | Increase of the number in the field of optoelectronics . | 5 |
| Figure I.2 | ZnO powder . | 7 |
| Figure I.3 | Representation of ZnO crystalline structures: (a) cubic rocksalt , (b) cubic zinc blende and (c) hexagonal wurtzite . | 8 |
| Figure I.4 | Elementary mesh of the wurtzite structure of ZnO . | 9 |
| Figure I.5 | ZnO electronic structure . | 12 |
| Figure I.6 | Size range of nanoparticles compared to major chemical and biological structures. | 16 |
| Figure I.7 | Types of nanoparticles by size . | 17 |
| Figure I.8 | Various ZnO nanostructures Note: Scale bar is not shown . | 17 |
| Figure I.9 | Cross-section view of a solar photocell . | 19 |
| Figure II.1 | "Top-down" and "bottom-up" synthesis of nanofabrication. | 25 |
| Figure II.2 | The sol state . | 26 |
| Figure II.3 | The gelificationstate . | 27 |
| Figure II.4 | Hydrolysis reaction . | 28 |
| Figure II.5 | Alcoxolation condensation reaction . | 28 |
| Figure II.6 | Oxolation condensation reaction . | 29 |
| Figure II.7 | Evolution of the viscosity of the solution and the elastic constant of the gel with the time. T _g is the time at which the soil-gel transition is reached. | 30 |
| Figure II.8 | The types of drying . | 31 |
| Figure II.9 | Applications of sol gel method . | 33 |
| Figure II.10 | Zinc acetate dihydrate and Citric acid monohydrate. | 34 |
| Figure II.11 | Various samples prepared in our work. | 37 |
| Figure II.12 | The flow chart of major steps in the development of a ZnO powder pure and doped. | 38 |
| Figure II.13 | The Principle of Bragg's Law. | 40 |
| Figure II.14 | The principle of operation of UV-visible . | 41 |
| Figure II.15 | Determination of E _g . | 43 |
| Figure II.16 | EVOLUTION 220 spectrophotometer image. | 43 |

| | | |
|---------------|---|----|
| Figure II.17 | The schematic representation of FTIR . | 44 |
| Figure II.18 | Thermo Scientific FTIR instrument (Nicolet 8400s). | 45 |
| Figure II.19 | Preparation of sample for description IR . | 45 |
| Figure III.1 | XRD patterns of ZnO pure powders. | 51 |
| Figure III.2 | XRD pattern of ZnO doped 3% Ga. | 52 |
| Figure III.3 | XRD pattern of ZnO doped 3% Bi. | 52 |
| Figure III.4 | Crystallite size and the strain as functions of dopage types. | 54 |
| Figure III.5 | The dislocation density as functions of doping type. | 55 |
| Figure III.6 | The transmittance spectra of ZnO pure and plots of $(\alpha h\nu)^2$ versus $h\nu$ of ZnO pure. | 57 |
| Figure III.7 | The transmittance spectra of 3% Ga doped ZnO and plots of $(\alpha h\nu)^2$ versus $h\nu$ of 3% Ga doped ZnO. | 57 |
| Figure III.8 | The transmittance spectra of 3% Bi doped ZnO and plots of $(\alpha h\nu)^2$ versus $h\nu$ of 3% Bi doped ZnO. | 57 |
| Figure III.9 | The transmittance spectra of 3% Ga+3%Bi doped ZnO and Plots of $(\alpha h\nu)^2$ versus $h\nu$ of 3% Ga+3%Bi doped ZnO. | 58 |
| Figure III.10 | Variation of the band gap with types of the doping. | 59 |
| Figure III.11 | FTIR spectra of ZnO pur and 3%Ga-doped ZnO and3%Bi-doped ZnO and 3%(Ga+Bi) -doped ZnO. | 60 |

List of Tables

| | | |
|-------------|---|----|
| Table I.1 | Main characteristics of the wurtzite structure of ZnO . | 9 |
| Table I.2 | ZnO Optical Properties . | 11 |
| Table II.1 | The physical and chemical properties of different chemicals used in this work. | 34 |
| Table II.2 | Value of time of charred tc per sample. | 37 |
| Table II.3 | Overview of experimental techniques needed to study the morphology, structure and properties of ZnO nanoparticles . | 39 |
| Table III.1 | A summary table of the structural parameters of dopage types. | 56 |
| Table III.2 | Lattice parameters of dopage types. | 58 |
| Table III.3 | Optical band gap values of undoped and doped ZnO. | 60 |

General Introduction

General Introduction

The synthesis of semiconductor nanoparticles is at the heart of the laboratory's activities, both with a view to a fundamental understanding of their growth and electronic properties, but also for their multiple applications, especially in large-area electronics and for pollution control. Research in the field of materials consists in imagining and designing new architectures offering better performance than already existing materials. Over the past twenty years, efforts have been focused in part on the development of nanomaterial, whether they take the form of particles, thin films or massive samples. Compared to conventional materials, nanomaterial present new physical properties that offer promising prospects in terms of application whether in the field of magnetism, mechanics, catalysis or optical [1].

The use of ZnO in nanotechnology is relatively new. Over the past fifteen years, the number of publications on this iono-covalent crystal has continued to increase and is the most competitive of transparent semiconductor oxides. It can crystallize under normal temperature and pressure conditions according to the wurtzite structure which is the most stable and preferred [2-4], and has been commonly used in its polycrystalline form for over a hundred years in a wide range of applications: facial powders, ointments, sunscreens, catalysts, lubricant additives, paint pigmentation, piezoelectric transducers, varistors, and as transparent conducting electrodes [3].

Doping is the most common strategy used to improve the quality of ZnO nanoparticles, first stabilizing the polar faces of its wurtzite crystallographic structure. Thanks to the excellent characteristics (optical, electrical and magnetic) of certain elements, especially Gallium and Bismuth, the nanostructures of the ZnO doped (ZnO: Ga -Bi) are widely used in the industry for several applications.

Several methods have been used to synthesize nanostructures of ZnO: Ga-Bi . These methods include the soil-gel process. The latter is most used because of the low cost[4]. We have written this brief in three chapters:

The first chapter devotes most of it to zinc oxide and gives the structural, physical, chemical and applications and advantages of zinc oxide.

The second chapter covers the definition of the Sol-Gel process and the most important steps followed, its various advantages and applications, as we mention the most important steps to prepare pure ZnO powders as well as Bi-doped and Ga-doped powders. Chapter II discusses the different characterization techniques used in this study.

The third chapter presentation and discussions the results obtained by the various characterization techniques: structural (XRD), optical (UV-Visible spectrophotometry), and chemical (IR).

This work ends with a general conclusion that highlights the major studies.

References

- [1] Mahcene F,(2021),Synthèse par Sol-gel et caractérisation structurale etoptique de nano poudres de ZnO pures et dopées en Aluminium (0.1, 0.5, 0.75, 1, 5, 7, 10, 15 et 20%), Doctoral dissertation, Université Frères Mentouri-Constantine 1.
- [2] DimitriH, (2013), ZnO nanostructuré: étude expérimentale de l'auto-organisation de nanoparticules et simulations numériques du dopage dans des phases expansées , Doctoral dissertation, Université Claude Bernard-Lyon I.
- [3] Bouaichi F, (2019), Deposition and analysis of Zinc Oxide thin films elaborated using spray pyrolysis for photovoltaic applications , Doctoral dissertation, University Mohamed Khider of Biskra).
- [4] Maache A, (2021), Elaboration et caractérisation optique des couches minces de ZnO dopé ou Co-dopé obtenues par méthode sol-gel , Doctoral dissertation, Université Ferhat Abbas - Sétif 1 .

Chapter I
Bibliographic studies

In recent years I have taken semiconductors (II-VI) like ZnO Center of attention and efforts of many researchers to the importance of this scientific topic and its various advantages and applications.

In chapter I we will address the main characteristics, applications and advantages of Zinc oxide.

I.1. Zinc Oxide «ZnO»

In the field of research materials with semiconductor properties, the first work undertaken on ZnO appeared in 1930 [1]. Zinc oxide is still today located in the fields of chemical industry and pharmaceutical (paints, sunscreens, etc...). By the 1920, ZnO was also used as a transducer in the receivers of the first wireless radios (effect piezoelectric).

ZnO has been extensively studied since the early 1950 before being relatively abandoned in the 1970. Since the 1990, there has been a significant resurgence in attention due to its highly fundamental attraction in the field of optoelectronics [2]. In this period (around 1990), there has been an increase in the number of publications on the ZnO (see figure I.1). More recent reviews were published about ZnO[3].

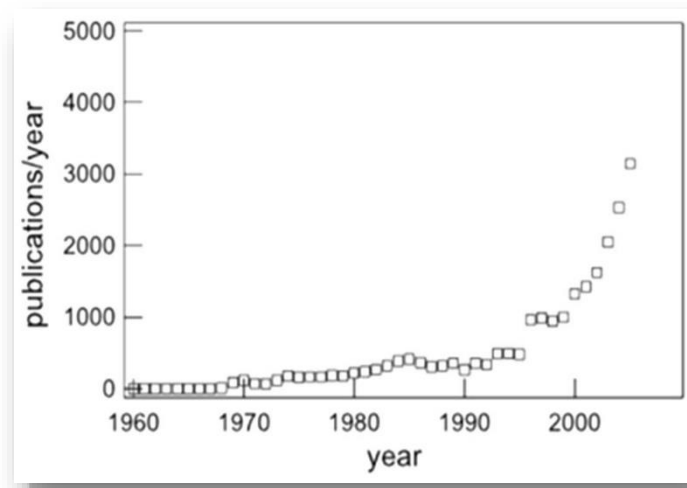


Figure I.1: Increase of the number in the field of optoelectronics [2].

I.2. Why choose ZnO specifically ?

ZnO is a wide band semiconductor prohibited (3.37 eV to 300K), it is transparent in the visible and near infrared (IR). It presents a set of properties that allow its use in a certain number of applications as per example varistances (electronic devices based on polycrystalline ceramic having nonlinear current-voltage characteristics), used to block

surges electrical. It can also find applications in optoelectronics, cathode luminescence, photoluminescence, electroluminescence, catalytic, for detection gases, or as a piezoelectric material, as well as other very varied uses.

Chapter I presents a general information on zinc oxide ZnO and gas sensors [4].

The main advantages of ZnO are[5] :

- High luminescent efficiency and non-ohmic, non-toxic.
- High excitation link energy (60 MeV)[6].
- ZnO can be prepared at a lower temperature[7].
- High piezoelectric effect ($e_{33} = 1.2 \text{ C/m}^2$).
- High thermal conductivity ($K = 0.54 \text{ W.cm}^{-1}.\text{K}^{-1}$).
- Drift mobility that saturates at higher fields than GaN (attractive for devices with high frequency).
- A very high shear module (45.5 Gpa) which indicates crystal stability (for example: 18.35Gpa for ZnSe, 32.6 GPa for GaAs, 51.37Gpa for Si).
- Very abundant on Earth.
- Enthalpy training is $6.5 \times 10^5 \text{ J.mol}^{-1}$.
- Melting temperature is greater than 2250 K.
- Its density is 5675 Kg.m^{-3} .

I.3. Properties of zinc oxide

In this paragraph we will address the mention of the most important characteristics of ZnO both physical (structural, optical, electronic, mechanical...) or chemical.

I.3.1. Physical Properties

ZnO has the following physical properties[3]:

 **Color:** Pure microcrystalline zinc oxide is white. Single crystal zinc oxide is colorless. Zinc oxide turns lemon yellow on heating and reverts to white on cooling (figure I.2).

- ✚ **Melting point** :Zinc oxide sublimates at atmospheric pressure at temperatures over 1200 C°. Under high pressure a melting point of 1975C° has been estimated.
- ✚ **Relative density** : 5.607
- ✚ **Heat of Sublimation** between 1350C° and 1500C°: -129 Kcal/mole (vapor not disassociated) and 193 KCal/mole (vapor associated).
- ✚ **Heat Capacity**: $C_p = 9.62 \text{ cal/deg/mol}$ at 25 °C.
- ✚ **Molecular weight**: 81.37 g/mol.
- ✚ **Vapor Pressure (1500 C°)**: 12mm.
- ✚ **Refractive index**: $w = 2.004$, $e = 2.020$.



Figure I.2: ZnO powder[8].

I.3.1.1. Structural properties of ZnO

Zinc oxide crystallizes into three different crystallographic structures depending on the condition of preparations [9]:

- Zinc Blende structure: is stable in high pressure (10 GPa) just by growth on cubic substrates (Figure I.3.b).
- Rocksalt structure: This structure is obtained at very high pressures (Figure I.3.a).
- The hexagonal structure Wurtzite: is more stable thermodynamic under the conditions.

In this work we study the compact hexagonal structure of the wurtzite type.

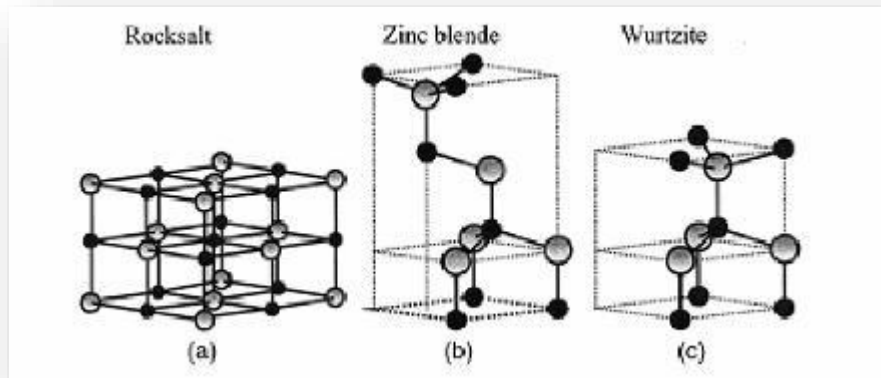


Figure I.3: Representation of ZnO crystalline structures: (a) cubic rocksalt, (b) cubic zinc blende and (c) hexagonal wurtzite[10].

I.3.1.1.1. ZnO Wurtzite Phase

The wurtzite structure has a hexagonal unit cell with two lattice parameters, a and c , in the ratio of $c/a=1.633$.

- Two Zn atoms occupying the sites: $(0, 0, 0)$ and $(1/3, 2/3, 1/2)$.
- Two O atoms occupying the sites: $(0, 0, 3/8)$ and $(1/3, 2/3, 7/8)$.

Each zinc atom is surrounded by four oxygen atoms at the tops of a tetrahedron. Zn crystallographic site actually sees , a tetrahedral ligand field with distortions along the c axis.

As a result, the zinc atom is not exactly at the centre of the tetrahedron but moved 0.11 \AA in the direction parallel to the axis [9].

ZnO primitive mesh, includes a polar plane (001) , and a plane $(0\bar{1}0)$ not polar (figure I.4), the cations of Zn^{+2} are represented in red, the anions of O^{-2} in violet. This structure allows zinc oxide to have piezoelectric properties. The mesh zinc oxide elemental has two ZnO patterns per mesh with a rate of filling of 0.48 [11].

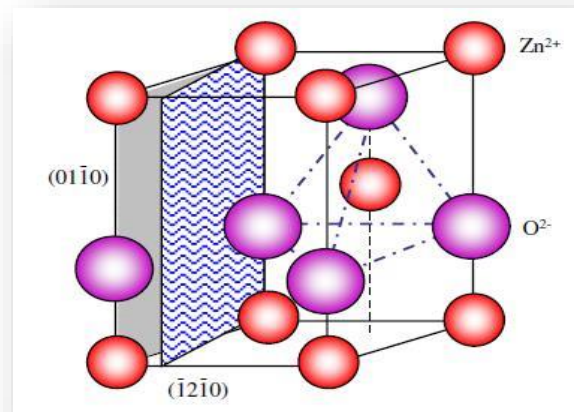


Figure I.4: Elementary mesh of the wurtzite structure of ZnO[11].

Indeed, the atoms of zinc and oxygen occupies only 40% of the crystal's volume, leaving empty areas of radius 0.95 Å. It is possible that, under certain conditions, excess zinc atoms could space, that is to say in an interstitial position. This feature allows explain certain specific properties of the oxide, related to the phenomena of semi conductivity, photoconductivity, luminescence, catalytic properties and solid chemical [12].

The table below presents a summary of some structural characteristics of zinc oxide.

Table I.1: Main characteristics of the wurtzite structure of ZnO[2].

| Network | | Hexagonal Würtzite |
|---|----------------------|---|
| Angle | | $\alpha=\beta=90^\circ \gamma=120^\circ$ |
| Lattice parameters (T=300K) | | $a_0=0.32495(\text{nm})$ $c_0=0.52069(\text{nm})$ $a_0/c_0=1.602$ (1.633 in an ideal wurtzite structure) |
| Atomic position | | $\text{Zn} : 2/3, 1/3, 0 ; 1/3, 2/3, 1/2$ $\text{O} : 2/3, 1/3, \mu ; 1/3, 2/3, 1/3+\mu$ and $\mu=3/8$ |
| Ionic ray for a coordination tetrahedral | Covalent bond | $\text{Zn neutral} = 1.31 \text{ \AA} \quad \text{O neutral} = 0.66 \text{ \AA}$ |
| | ionic bond | $\text{Zn}^{+2}=0,06 \quad \text{O}^{-2} = 1,38 \text{ \AA}$ |

| | |
|--|---|
| Distance between O^{2-} and Zn^{+2} (most close neighbours) | According to axis c $d=1.96\text{\AA}$,For the other three of 1.98\AA |
| Crystalline ray for coordination Tetrahedral | $Zn^{+2}=0,74\text{\AA}$ $O^{2-}=1,24\text{\AA}$ |

I.3.1.1.2. The different types of defaults in the ZnO

The defects in ZnO depend on the growth method and the conditions under which this material is produced. The following defects may be listed [13]:

- ✚ Spot defects (interstitial, gap, foreign atoms).
- ✚ Linear defects (dislocations and grain seams).
- ✚ Flat defects (grain joints).
- ✚ There are other types of thermal (Phonon) or electrical defects (electrons, holes, excitons, etc...).

I.3.1.2. Electrical properties

The concentration of free carriers is on average about 10^{16} cm^{-3} , it can reach 10^{20} cm^{-3} for ZnO type n and 10^{19} cm^{-3} for ZnO type p, so ZnO has a high conductivity. However, ZnO type p remains highly questionable and has not been tested experimentally [14]. Electronic mobility may exceed $1000\text{ cm}^2.\text{V}^{-1}.\text{s}^{-1}$ if the surface condition effect is eliminated[15].

The excitonic binding energy is 60 MeV to 300K, this is one of the reasons for which ZnO is highly coveted, especially for making devices optoelectronics at room temperature. The mobility of electrons corresponding to the effect hall at 300K for low conductivity type n is $\mu=200\text{ cm}^2.\text{V}^{-1}.\text{s}^{-1}$, and for low conductivity type p, it varies between 5 and $50\text{ cm}^2.\text{V}^{-1}.\text{s}^{-1}$ [14-15].

Doping, whether substitutional or interstitial, of the ZnO layers makes it possible to obtain and improve the conductivity of type n, generally obtained by an excess of zinc in the ZnO layers. In addition, ZnO can give non-ohmic behavior, which makes it a very good competitor for the manufacture of varistances[14].

I.3.1.3. Optical properties

The interaction of light (electromagnetic wave) with matter (electrons of the material) can clearly explain optical properties of a material.

The optical properties of zinc oxide have been studied by several techniques. They concern the study of optical absorption, transmission, reflection, photoluminescence or the optical gap.

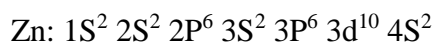
Zinc oxide is a transparent material in the visible. It makes part of the family of transparent semiconductor oxides and has high absorption and diffusion in the ultra-violet range [2].

Table I.2: ZnO Optical Properties [14].

| Properties | Value |
|----------------------------|-----------------------|
| dielectric constant | $\epsilon = 8.7$ |
| absorption coefficient | 104 cm^{-1} |
| Refractive Index at 560 nm | 1.8-2 |
| Refractive Index at 590 nm | 3.13-2.029 |
| Width of excitonic band | 60 meV |
| Transmittance | >90% |

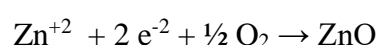
I.3.1.4. Electronic band structure

It is recalled that the electronic oxygen and zinc band structures are :



ZnO is composed of zinc and oxygen, these two elements belong to the columns II-VI respectively of the periodic table of chemical elements [16]. Figure I.5 shows that ZnO is a direct gap semiconductor. Minimum range of delivery (Zn cases) and maximum parity range (case sp of O) corresponds to the Γ point of the Brillouin region (which corresponds to the $k = 0$ point in mutual space). Then the electronic shifts are in ZnO directly [17].

The zinc oxide formation reaction is [2]:



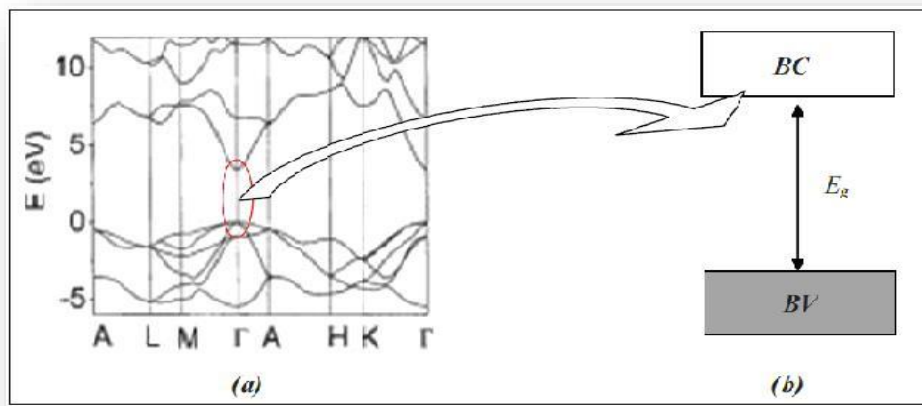


Figure I.5: ZnO electronic structure [17].

I.3.1.5. Mechanical properties

Zinc oxide is a relatively soft substance with hardness of about 4.5 degrees on the mousse scale. These flexible constants are smaller than those related to III-V semiconductors such as gallium. Zinc oxide has a very long light life. It is one of the halves or semi-vectors with the highest electro-compressive intensity that can be compared with gallium, this special makes it an important material from the technological side of a number of applications [18].

It has been indicated that ZnO has the larger piezo-electric tensor, or at least one comparable to GaN and AlN, this property actually makes it a technologically important material for many piezoelectric applications, which require a large coupling electro mechanical[13].

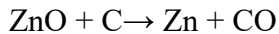
I.3.2. Chemical Properties

ZnO has the following chemical properties [19]:

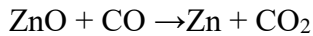
- ZnO occurs as the mineral zincite or as white powder known as zinc white. It is usually orange or red in color due to manganese impurity.
- Crystalline zinc oxide is thermochromic, which changes from white to yellow colour when heated and reverting to white colour on cooling. This change in colour is caused by a very small loss of oxygen at high temperatures.
- ZnO decomposes to form zinc vapor and oxygen at about 1975 C°, indicating its

considerable stability. Heating with carbon converts ZnO into Zn, which is more

volatile.



- The following reaction is extremely important in zinc pyrometallurgy.



- Commercial zinc oxide shows a measurable but low level of water solubility 0.005 g/litre.

I.3.3. Catalytic properties

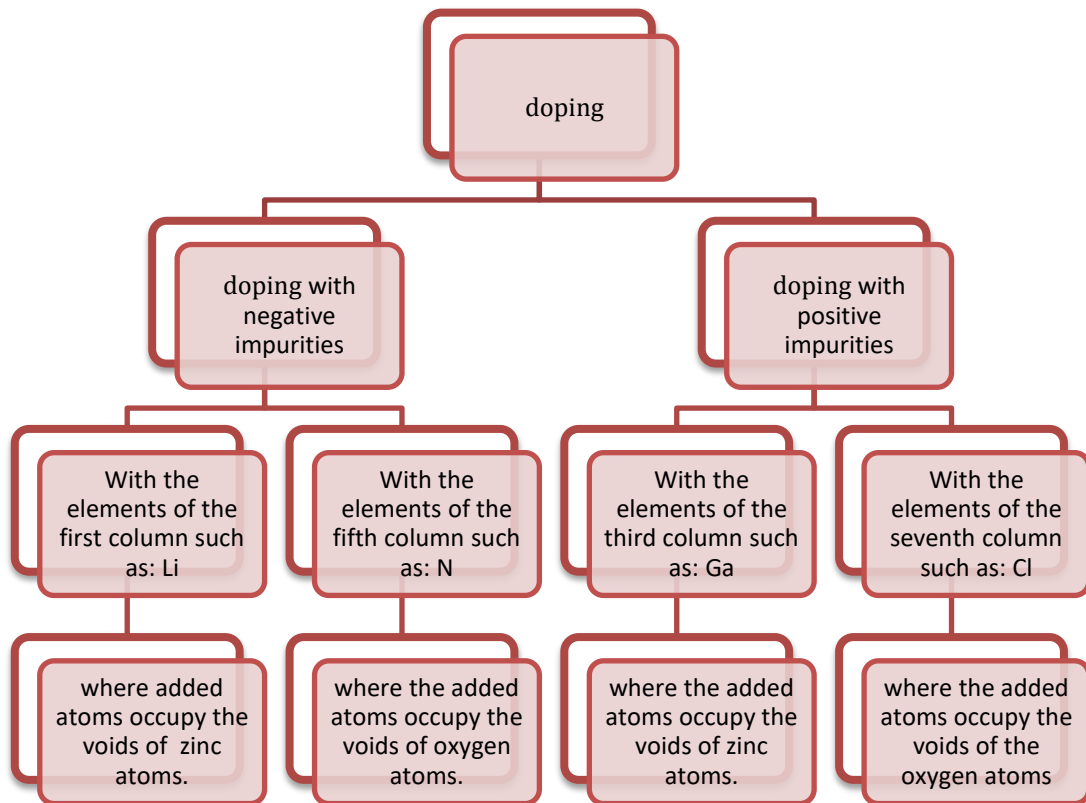
ZnO has interesting chemical properties especially that of absorption of surface. One of the possible applications concerns the capture and chemical capture of gas (H_2S , CO_2 , O_3 , H_2 and CH_4) or moisture. ZnO also has properties very promising catalysts due to the efficiency of the oxidation process. Powders suspended in water play an essential role as photochemical catalyst for reactions oxidation of oxygen to ozone, oxidation of ammonia to nitrate, degradation of organic pollutants (pesticides, dyes, etc...) or oxidation of phenols .

Like all catalysts, the efficiency of ZnO in a system depends essentially on its synthesis method, its crystalline network, its surface properties, its chemical nature and doping (electronic gaps, interstitial defects, atoms in an interstitial position, etc...), these numerous physico-chemical properties make ZnO a material particularly interesting in the field of photocatalytic degradation of pollutants organic [7].

I.4. ZnO doping

The addition of some impurities to the semi-pure vector called grafting or doping. These impurities create new energy levels that fall into the prohibited gap between the Conduction bande (BC) and valence bande (BV)[20].

Doping is divided into two parts[18]:



Forme I.1: Illustration of the types of doping

ZnO is characterized by high resistance that hampers it from good electrical transport, leading to the reduction of the latter. To this end, group 3 of the periodic table is used of which the most important Ga, In, etc.... So that we note the significantly increased conveyor, this property is the reason why ZnO restaurant is used in the solar cell industry with high permeability [21].

I.4.1. Doping with Bi

This type of vaccination is used especially in the field of variable resistors where ZnO acquires very important electrical properties including non-linear electric conveyor[21]. This allows its wide use in the protection of electronic devices, particularly in stations high voltage electrical[17].

I.4.2. Doping with Ga

Gallium affects[22]:

- ✚ The crystal composition of ZnO, where a new phase its formula $ZnGa_2O_4$.
- ✚ Electric properties where we observe an increase in electric conveyor .

- ✚ Optical properties it gives a large light permeability of 85% for light and is more influential compared to Al, In .

I.5. Nanomaterials

In the word nano particle the term nano means (10^{-9}) meter, nano particles are formed by not more than 10^6 atoms, their properties are different to those of the same atoms bound together to form massive materials. They are generally considered to be a number of atoms or molecules connected with a radius of less than 100nm. Seen as a subdivision of the material we can practically define them as an aggregate or a set of atoms whose dimensions are between 1 and 100nm[22].

I.5.1. Nanoparticles

A nanoparticle or an ultra-fine particle is the most fundamental component in the manufacture of a nano structure. It is defined as being a nano object whose decreases are reduced to the nanoscale. Its estimated size between 1-100nm (figure I.6).

In other words, a particle may consist of 10 to 10^6 atoms or molecule. The shape of the particles does not matter in this definition. The nanoparticles possess particular physico-chemical properties, this is due to part of the number of atoms on the surface which is not negligible in relation to that present in the core of the particle. In these conditions, it is obvious that the surface plays a role knowledge of the properties of nanoparticles. II-VI semiconductors in nanometric form, have electronic properties and optics that differ from those of the microcrystal by the fact of quantum confinement of electronic excitations in a reduced volume: this is an area of dimensions for which we observe the passage of the properties of solid crystal to that of the molecule [11].

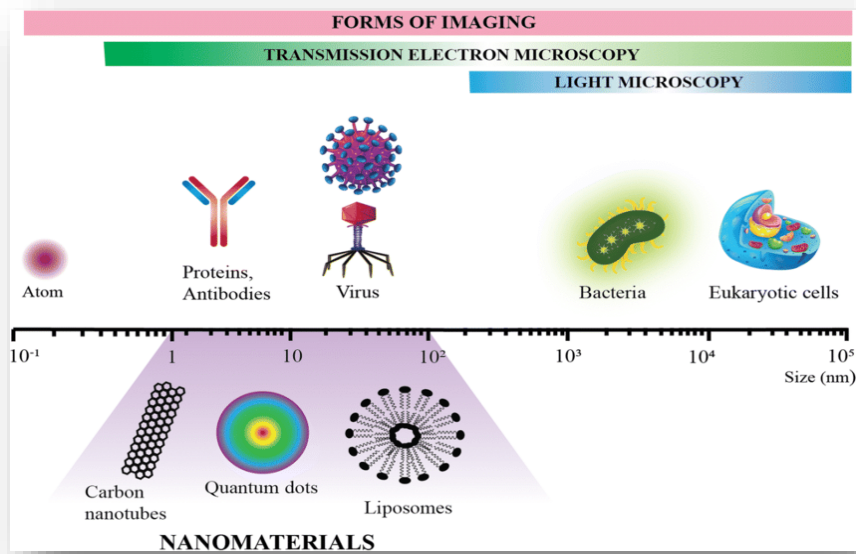


Figure I.6: Size range of nanoparticles compared to major chemical and biological structures [23].

I.5.2. Classification of nanomaterials

Nanomaterials can be classified into four families according to their uses (Figure I.7):

- ✚ **Materials of dimension 0:** Materials in dispersed, random or organized form (nanoparticles) as in colloidal crystals for optics or magnetic fluids, they can be composed of a few tens to a few thousand atoms.
- ✚ **Materials of Dimension 1:** Materials in the form of nanowires or nanotubes... of which the nanometric dimension concerns the diameter.
- ✚ **Materials of Dimension 2 :** Materials in the form of a thin layer deposited on a solid material (substrate), as in aggregate deposition or thick coating obtained by plasma projection or electrochemical pathway.
- ✚ **Materials of dimension 3 :** Materials in compact form in ceramics and nanostructure metals [24].

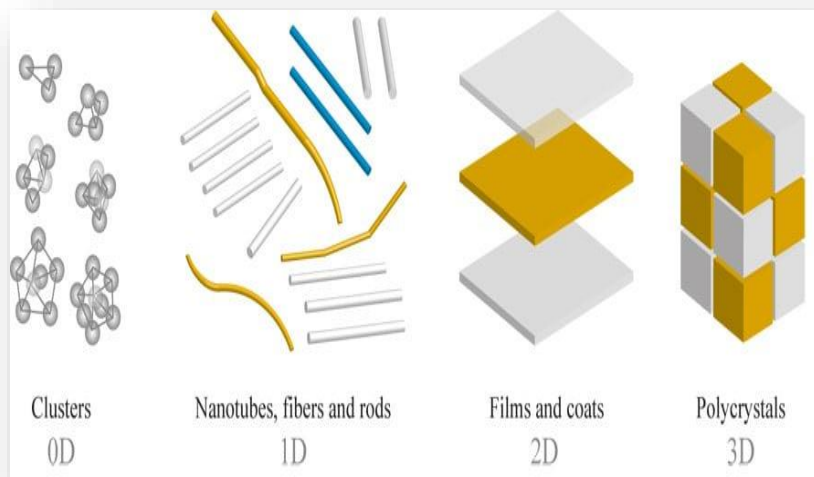


Figure I.7: Types of nanoparticles by size [25].

Figure I.8 shows nanostructures made by thermal evaporation of ZnO powder by controlling the kinetics.

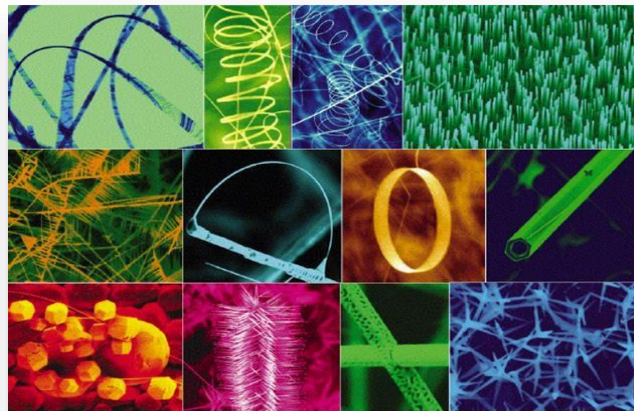


Figure I.8: Various ZnO nanostructures Note: Scale bar is not shown [3].

I.6. Applications of zinc oxide

ZnO has a diverse range of applications. Due to its reactivity, ZnO is an excellent precursor for obtaining other Zn compounds. ZnO has proven to be a boon to materials science because of its various advantages, for instance: UV absorption, antimicrobial capabilities, and steady thermal and optical properties. ZnO has made a substantial contribution to ceramics, lubricants, ointments, adhesives, and the rubber sector [2].

I.6.1. ZnO powder applications

No industrial sector will be left out of the Nano revolution. ZnO has applications in the medical sector, prostheses based on bio-nonmaterial's and drug carriers to target and treat diseases. Surface nonmaterial's provides solutions to improve system performance energy and developing clean energy. Examples include carbon nanopowders for fuel cells, nanotubes for hydrogen storage. The miniaturization and integration in the field of information technologies are important issues involving nonmaterial's. Current and potential applications of these nonmaterial's are extremely varied and can be found in all fields, from magnetism to optics to catalysis, batteries, the environment, mechanical etc...[11].

It also enters the ceramics industry, in used in the manufacture of glass, porcelain and sinters, as it decrease the coefficient of expansion and improve stability in tension , it can also for the manufacture of varistances because, in the presence of small quantities of metal oxides (bismuth, praseodymium), zinc oxide has excellent properties of electric nonlinearity. This allows it to be widely used in the protection of electronic devices, particularly in electrical stations high voltage [26].

The ability to absorb UV light makes zinc oxide a candidate for choice for sunscreens. Many metal oxide type materials are used in the formulation of cosmetic products (cream, foundation, nail polish), curative (hygiene and care products) or preventive (sunscreen) [27].

I.6.2. ZnO applications in thin film

I.6.2.1. Solar Cells

The latter has made spectacular progress especially in recent years gives the corresponding shape to the solar cell infrastructure based on the thin layers of ZnO (see figure I.9).

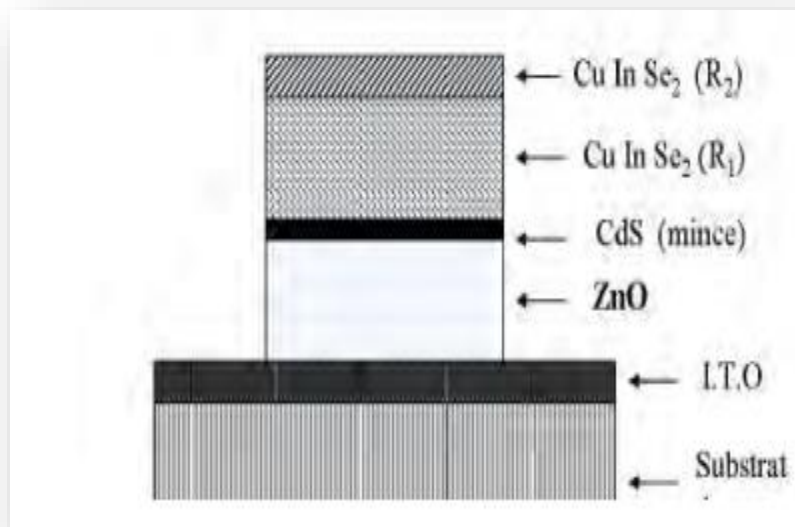


Figure I.9: Cross-section view of a solar photo cell [9].

I.6.2.2. Light emitting diodes

The principle of light emitting diode (LED) consists in converting electrical energy to light energy like gallium nitride and thanks to its wide band prohibited (3.37 eV), also finds its place in the realization of light emitting diodes emitting especially in blue and UV.

These two materials have similar properties, but ZnO has some advantages over GaN. We can mention for example its large binding energy of the exciton (60 MeV against 21 MeV for GaN), giving it potentially good light emission capabilities at room temperature[9].

I.6.2.3. Gas sensor

Zinc oxide is a semiconductor with large gaps where its conductivity depends on the nature of environmental gas. Thus, the presence of a reducing gas (CO, H₂) will cause an increase in the electrical conductivity of thin layers of ZnO, while the presence of an oxidizing gas will result in a reverse behavior. In effect the performance of a gas sensor (sensitivity, selectivity, stability, reversibility, recovery and reputability) are closely related to the materials used, be it their composition, morphology or surface. Because of its chemical properties, zinc oxide becomes a good candidate for gas detection. Zinc oxide based gas sensors were used for detection nitrogen dioxide or carbon monoxide. Other ZnO-based gas sensors high sensitivity and excellent selectivity for dim ethylamine and triethylamine amino gases [9].

I.6.2.4. Varistors

ZnO varistors have now been in widespread use for more than 30 years. The technology has supplanted generally less useful prior approaches to voltage surge protection such as silicon carbide arresters, gas discharge tubes and to some extent semiconductor-based surge suppressors such as Zener diodes. A significant advantage of ZnO varistors as a transient protective device derives from the ceramic nature of the material. Since the material is polycrystalline with energy absorption occurring essentially at the grain boundaries distributed throughout the volume of the material, ZnO varistors are inherently able to absorb more energy than single-junction protective devices such as Zener diodes[28].

I.6.2.5. Medical

ZnO nanopowders are known for their ability to create reactive oxygen species(ROS) and trigger apoptosis, like other metal oxide nanopowders, offer great medicinal potential. ZnO nanopowders are use ful as anticancer, antibacterial, and antifungal agents because of their properties. When loaded and given with other medicinal regimens, ZnO nanopowders have been shown to have synergistic benefits. Targeted drug delivery and clinical diagnostics are becoming more common as ZnO nanopowders are a type of nanomaterial that has a lot of applications in medical purposes and green technologies, and they can be safely manufactured at a cheap cost[29].

References

- [1] Miller P H, The electrical conductivity of zinc oxide , University of Pennsylvania, Philadelphia, Pennsylvania Phys. Rev, 60, 890 (1941).
- [2] Boudiaf Y R., (2020), Elaboration et Caractérisation des nanopoudres de ZnO pure et dopées avec le Ga par la méthode sol-gel, Mémoire master. Université Mohamed Khider of Biskra.
- [3] Naza IH ,Redjough N E H,(2022), Elaboration of pure and Bi-doped ZnO nano-powders with the sol-gel method. Mémoire master . Université Mohamed Khider Biskra.
- [4] Bakha Y, (2013), Propriétés optoélectroniques de l'oxyde de zinc préparé chimiquement, phénomènes d'adsorption et application à la détection des gaz, Thèse de Doctorat Science, Université des Sciences et de la Technologie d'Oran .
- [5] <https://www.zinsa.com/en/blog/zinc-oxide-applications-uses>.
- [6] Bouaichi F, (2019), Deposition and analysis of Zinc Oxide thin films elaborated using spray pyrolysis for photovoltaic applications ,Doctoral dissertation, University Mohamed Khider of Biskra.
- [7] Maache A, (2021), Elaboration et caractérisation optique des couches minces de ZnO dopé ou Co-dopé obtenues par méthode sol-gel ,Doctoral dissertation. Université Ferhat Abbas - Sétif 1 .
- [8] Won Il P, Jin Suk K, Gyu-Chul Y, Bae M H, Fabrication and electrical characteristics of high-performance ZnO nanorod field-effect transistors, University of Science and Technology (POSTECH), Pohang, Gyeongbuk 790-784, Korea 85(21),(2004).
- [9] Mekhloul M, (2021), les propriétés électriques et optiques des nanopoudres de ZnO pur et dopé en Ga élaborés avec la méthode Sol gel, Mémoire master . Université Mohamed Khider Biskra,.
- [10] Aida M S, Bouhssira N. (2017). Elaboration des films minces d'oxyde de zinc par évaporation et par pulvérisation magnétron et étude de leurs propriétés. These doctorah. Université Constantine 1.
- [11] Bekhti W, (2015), Synthèse par voie hydrothermal et caractérisation des micro/nanostructures d'oxyde de zinc. Thèse doctorat . Université Oran 1.
- [12] زناتي ك , (2016) , دراسة خصائص الأغشية الرقيقة لأكسيد الزنك الغير مطعم والمطعم بالالمنيوم والمغنيزيوم المحضرة بتقنية صول-جل , مذكرة ماستر , جامعة العربي بن مهيدي ام البواقي .

- [13] Abd-Elmağsoud I G, Elsaadawi H A, Ahmed A I, Abdel Khalek A, Arisha A. (2022). The Vast Biomedical Applications of Zinc Oxide Nanoparticles. Zagazig Veterinary Journal, University in Cairo (BUC) , Egypt ,50(3), 201-218.
- [14] Adachi S ,(2005). Properties of Group-IV, III-V and II-VI Semiconductors, John Wiley and Sons,Ltd,West Sussex, England.
- [15] Walters A B, Liu C.-C,Vannice M.A, (2000), Distinguishing surface and bulk electron charge carriers for ZnO powders, J. Molecular Catalysis A: Chemical 162,287–29.
- [16] SrikantV,Clarke DR,On the optical band gap of zinc oxide, Journal of Applied Physics, University of California, Santa Barbara, California ,83 5447-5451, (1998).
- [17] Bencherif N, (2014),Synthese caracterisation des films de ZnO pur et dope a l'Indium par la technique de spray pyrolyses ultrasonique, Doctoral dissertation , Université d'Oran.
- [18] Hamrit S, Djessas K. (2017). Optimisation des dépôts sur des substrats flexibles d'oxydes transparents conducteurs nanostructurés à base de ZnO , Doctoral dissertation Université de jijel.
- [19] Behera O, (2011), Synthesis and Characterization of ZnO nanoparticles of various sizes and Applications in Biological systems, Doctoral dissertation.Orissa, India
- [20] Bouchebbah H, Rabiai K, Djouadi D, (2021), Caractérisations de nanostructures de ZnO élaborées à différentes pressions et températures ,Doctoral dissertation, Univer. Abderrahmane Mira.
- [21] Boussafeur M, Hadjéris L, (2012), Elaboration par spray pyrolyse et caractérisations structurales de couches minces d'oxyde de zinc, Universite Larbi ben mhidi .Oum El Bouaghi.
- [22] Lahmani M, BréchnignacC, HoudyP, Nanomatériaux et nanochimies, ed. Echelles. 2006,Paris.
- [23] Boumezoued A, (2020). Etude et préparation par Sol-Gel de nanomatériaux à base d'oxydes semiconducteurs et leurs applications ,These doctorah. Universite Larbi ben mhidi .Oum El Bouaghi.
- [24] Delerue C, Lanno M, Nanostructures – Theory and Modeling .Nanosci. Technol. Springer Berlin Heidelberg, 2004.
- [25] Weast R C, Handbook of Chemistry and Physics, CRC PressLLC, 2000 N. W. Corporate Blvd., Boca Raton, FL 33431.1975.
- [26] Lionel L, Zinc oxide varistors. Magazine .American Ceramic Society Bulletin 6565(4), 639-646, 1986.

[27] قاديي, دراسة تأثير السترونتيوم على خصائص الشرائح الرقيقة لأكسيد الزنك, (2018), مذكرة ماستر, جامعة الوادي .

[28] ثابت ن, بولعراس ن, (2017), تحضير و دراسة الخواص البلورية و التحفيزية لمساحيق الأكاسيد النانوبلورية, مذكرة ماستر. جامعة الاخوة منتوري. قسنطينة.

[29] Poh TY, Ali N A T B M, Mac Aogáin M, Kathawala M H, Setyawati M I, Ng K. W , Chotirmall S H , Inhaled nanomaterials and the respiratory microbiome: clinical, immunological and toxicological perspectives. Particle and fibre toxicology, 15, 1-16. 2018.

Chapter II

methods and materials

In the first part of the chapter II we address the definition of the Sol-Gel process and the most important steps followed, its various advantages and applications, as we mention the most important steps to prepare pure ZnO powders as well as the Bi-doped and Ga-doped. The second part of the chapter II deals with the different characterization techniques used in this study.

II.1. Methods of synthesis of nanomaterials

There are two main approaches to forming nanoparticles: top-down and bottom-up (figure II.1).

- ✚ The first is to reduce the size from a solid material. It generally includes physical processes such as crushing (HEBM: high energy ball milling) but also, for example, evaporation/condensation techniques.
- ✚ The second is to construct nanomaterial atom by atom molecule by molecule or aggregate by connection. These nanomaterial are then used directly or serve as elemental meshes to create more complicated nanostructures than the first. It is thus mainly a matter of chemical processes, among which one can cite, for example the synthesis by solution-gelification (Sol-Gel) [1].

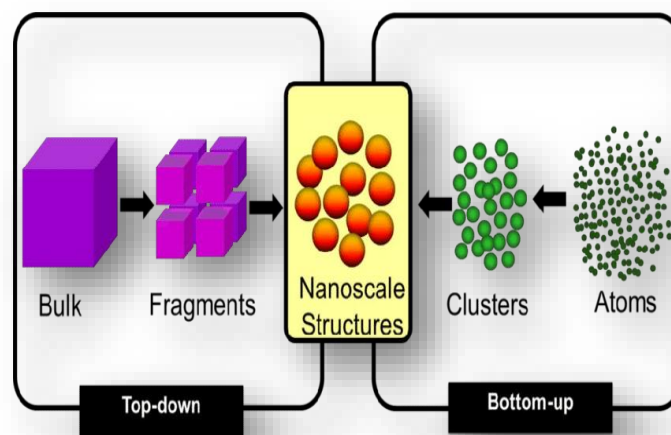


Figure II.1: "Top-down" and "bottom-up" synthesis of nano fabrication[2].

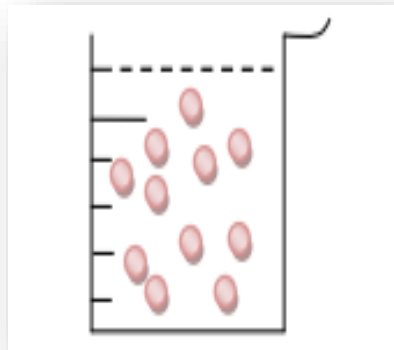
II.2. The sol-gel method

Sol-gel chemistry is the preparation of inorganic polymers or ceramics from solution through a transformation from liquid precursors to a sol and finally to a network structure called a gel [3], it was first described by chemist Ebelmen in 1845 (the formation of a solid glass from

silicic acid exposed to humid air). After a century the German firm Shott-Glaswerke and for the first time uses the sol-gel process to industry [4].

Sol-gel technology is an interesting research area of scientific and technological perspectives[5], this process is typically used to prepare metal oxides via hydrolysis metal precursors used as reagents in the production of hydroxide corresponding. The condensation of these hydroxides by removal of water produces a network of metallic hydroxide. When the whole function of hydroxide is linked, the freezing is completed and a porous gel is obtained. Removal of solvent molecules and proper drying of the gel allows the production of an ultrafine powder of metallic hydroxide. Subsequent heat treatments of this metal hydroxide gives an ultrafine powder corresponding to the desired metal oxide [6].

✚ **Sol:** the solution abbreviation is a colloidal Suspension consisting of a solid phase, granulometry between one nanometer and one micrometer, dispersed in a liquid. The rheological stability of this dispersion is generally ensured by the presence of a electrical surface load imposed by the catalytic conditions of the medium reactive (stability by electrostatic effect)(see figure II.2) [7].



FigureII.2: The sol state[1].

✚ **Gel:** is an intermediate state between a liquid and a solid, which is formed from a sol by increase in dispersed concentration(see figure II.3). The sol-gel transition is accompanied increased viscosity, creating a three-dimensional network that will trap the solvent [7].

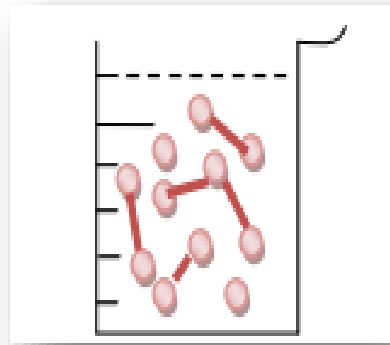


Figure II.3: The gelification state[1].

II.2.1. Ways of the Sol-Gel process

Depending on the nature of the precursors, molecular used in sol preparation, i.e. metal salts in aqueous solutions or metal alcoholates in organic solvents, two ways of the sol-gel process can be distinguished: colloidal (or inorganic) and polymeric (or metallo-organic) pathway[1].

II.2.1.1. Inorganic or colloidal route

Obtained from the dissolution of salts metal (chlorides, nitrates, oxychlorides, halides, etc..) in an aqueous solution. This inexpensive method is still very little used because it is difficult to control. It remains privileged for obtaining ceramic materials[4].

II.2.1.2. Metallo-organic or polymeric pathway

Obtained from metal alcoxides of formula $M(OR)_n$, where M is a metal atom of valence n (M= Si, Ti, Zr, Zn, Co, etc..) and R an alkyl organic group (C_nH_{2n+1}), and acetates or carboxylates (R-OH) in organic solutions. This polycondensation mechanism leads to a homogeneous and transparent gel. This very expensive method allows a better control of the reaction mechanism. The organic way is the way adopted and will be developed in this manuscript. Regardless of the synthesis and depending on the application, the gels must be dried afterwards to remove the solvents. This drying can be carried out under atmospheric or supercritical conditions in order to obtain xenrogals or aerogels respectively [4].

The Sol-Gel reaction is done in two stages: the synthesis of the «sol» then the formation of the «gel».

II.2.2. Predominant chemical reactions

The predominant reactions can be broken down into two categories [8]:

II.2.2.1. Hydrolysis reaction

This reaction is accompanied by a consumption of water and a release of alcohol. The solution thus obtained is called sol.

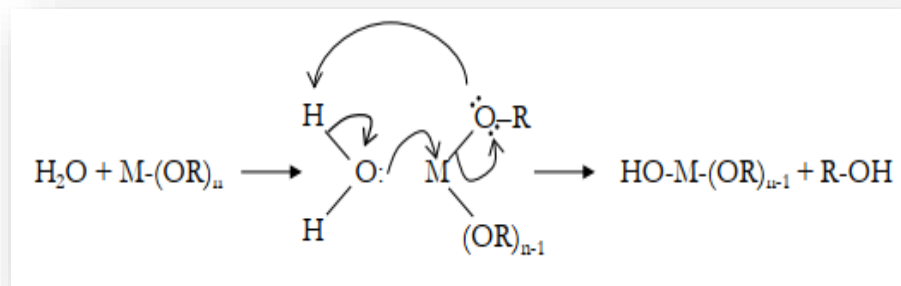


Figure II.4: Hydrolysis reaction [9].

II.2.2.2. Condensation reaction

The condensation reaction leads to the formation of a gel whose viscosity increases over time, this gel contains solvents and precursors that have not yet reacted. Two mechanisms enter into competition:

✚ Alcoxolation :

Consists in forming an oxygen bridge M-O-M between two metallic atoms while releasing an alcohol molecule.

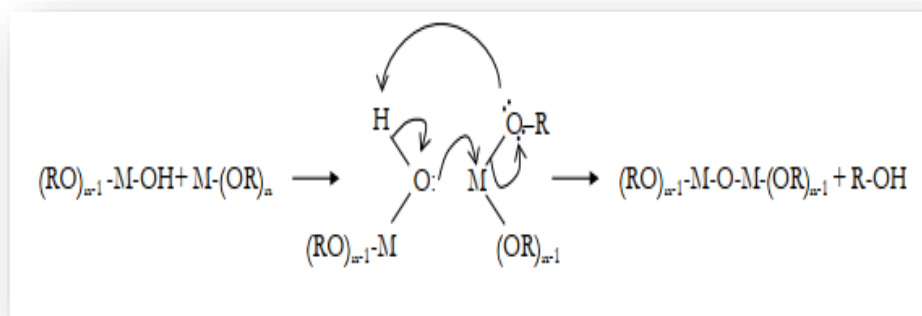


Figure II.5: Alcoxolation condensation reaction [9].

✚ Oxolation:

Consists in forming an M-O-M oxygen bridge between two metallic atoms leading to dehydration.

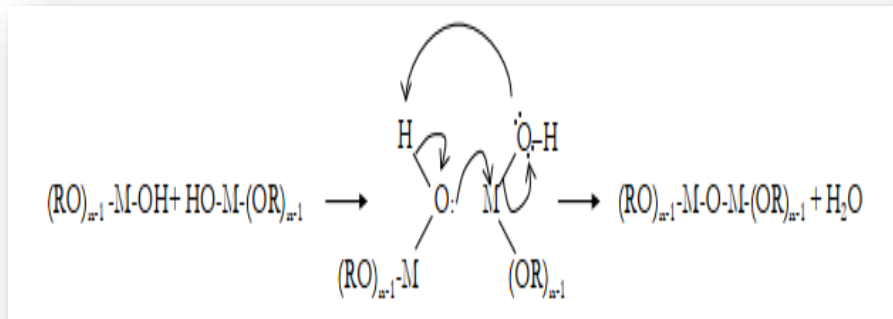


Figure II.6: Oxolation condensation reaction [9].

II.2.3. The sol-gel transition

The pattern generally adopted for gelification is that of growing polymeric chains agglomerating by condensation and forming clusters. During the advancement of hydrolysis and condensation reactions, polymeric clusters, whose size grows with time, are created. When one of these clusters reaches an infinite dimension (i.e. practically the size of the container). The viscosity also becomes infinite. The infinite cluster called the 'gel fraction' continues to grow by incorporating smaller polymeric groups. When all bindings have been used, the gel is formed. It results in divergence of the viscosity of the solution and growth of the elastic constant (or Coulomb module) in the freezing phase [10]. Figure II.7 shows the evolution of the viscosity of a soil and that of its Coulomb module, as a function of time.

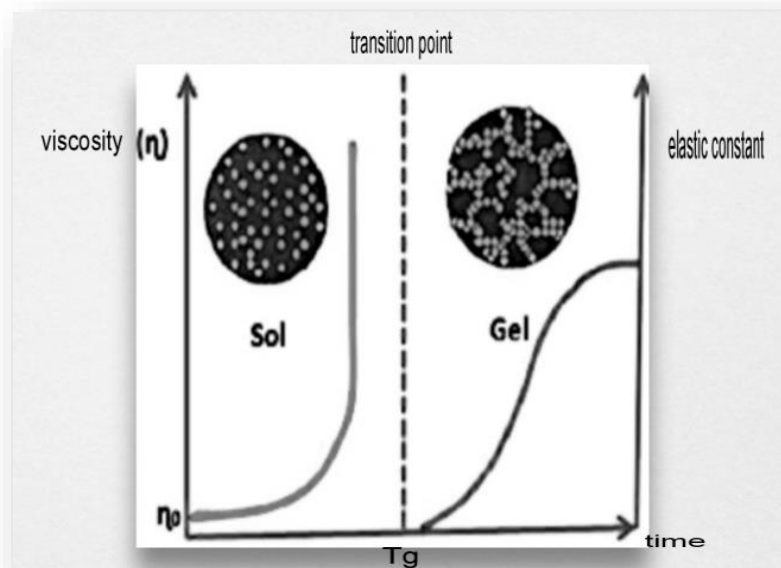


Figure II.7: Evolution of the viscosity of the solution and the elastic constant of the gel with the time. T_g is the time at which the soil-gel transition is reached[6].

II.2.4. Study of gelification time

The time of gelification noted t_g can vary significantly with depending on the initial composition. It can be determined experimentally by optically observing the viscosity of the soil. The gelification time t_g varies greatly from one sample to another, ranging from a few hours to several tens of hours at 70°C . It decreases with sample dilution.

As we can easily imagine, the gelification time depends on the incubation temperature. The increase in temperature produces a decrease of t_g and vice versa. T_g study at different temperatures can be used to calculate energy apparent activation of the aggregate percolation process or gelification. If gelification is kinetically controlled [11].

II.2.5. Drying

There are several types of drying [12].

II.2.5.1. Xerogel

Conventional drying (normal evaporation) leading to a reduction of volume ranging from 5 to 10%.

II.2.5.2. Aerogel

Drying under critical conditions (in pressure autoclave high) with little or no volume shrinkage (see Figure II.8).

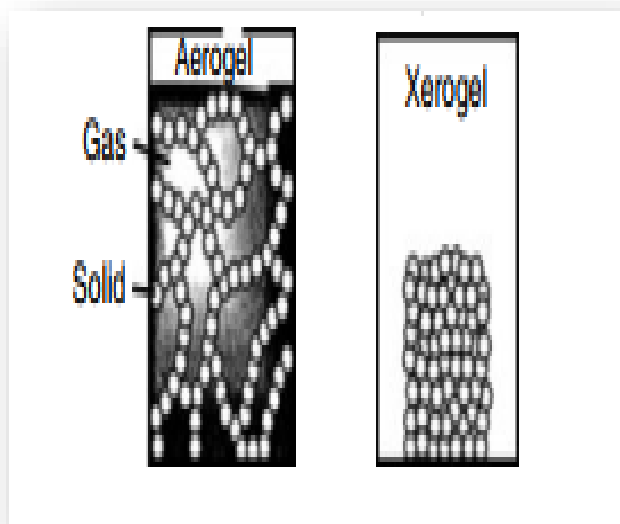


Figure II.8: The types of drying [13].

II.2.6. Parameters influencing the kinetics of reactions

✚ The temperature

This is the first parameter to consider which intervenes in any chemical reaction. In our case, it has an influence on the rates of hydrolysis and condensation preparation of the soil, then during aging or storage. Obviously, the more high, the faster reactions [14].

✚ The choice of alcoxide and its concentration

This choice is made according to the reactivity of the alcoxide, and the type of sample that we want to develop. Monitoring the hydrolysis reaction poses more problems, especially with alcoxides of transition metals with which can go up to the precipitation of hydroxide if special precautions are not taken[14].

✚ The solvent

The alcohol helping to avoid possible reactions between the various components which may modify the kinetics of reactions. The starting solvent is therefore generally alcohol. The water required for hydrolysis is only introduced in controlled and limited quantities [9].

✚ Soil pH (choice of catalyst):

An acid pH accelerates hydrolysis reactions and leads to a polymeric solution. Under acid catalysis, the formed gel is called polymeric gel, which has an open structure. Unlike acid pH, a basic pH promotes condensation reactions and the formation of three-dimensional species. The gel formed in this case is called colloidal gel and has a large pore structure (clusters) [9].

II.2.7. Advantages and disadvantages of sol-gel

The main advantages of the sol-gel method are[1]:

- ❖ Better purity.
- ❖ A better homogeneity.
- ❖ A very small particle size distribution (nanoscale).
- ❖ Lower preparation temperatures, instead of going through fusion, with others methods.

- ❖ The possibility to deposit on substrates of large size and complex shape.
- ❖ Adaptation of several shapes such as: thin layers, powders monolith and fibers.
- ❖ We obtain totally original materials, organo-mineral hybrids, of real nanocomposites, in which organic and metallic species are mixed at the molecular level [15].

However, disadvantages hinder the development of the sol-gel process:

- ❖ The high price of synthetic precursors.
- ❖ Sol-gel processes are not competitive for the production of large powder.
- ❖ The problem of handling large quantities of solvents.
- ❖ Certain chemical compounds are hazardous to human health [16].

II.2.8. Applications of Sol Gel method

The sol-gel technology is very efficient in producing various functional materials in which particle size, porosity, thin layer thickness, separation of particles with different compositions and structures may be controlled and successful applications have been achieved. Following the analysis of Sakka they may be summarized in a scheme (Figure II.9) where examples of materials applied in, electronics, optics, photonics, high-temperature technologies, chemical technologies, biochemistry and medicine are given [17].

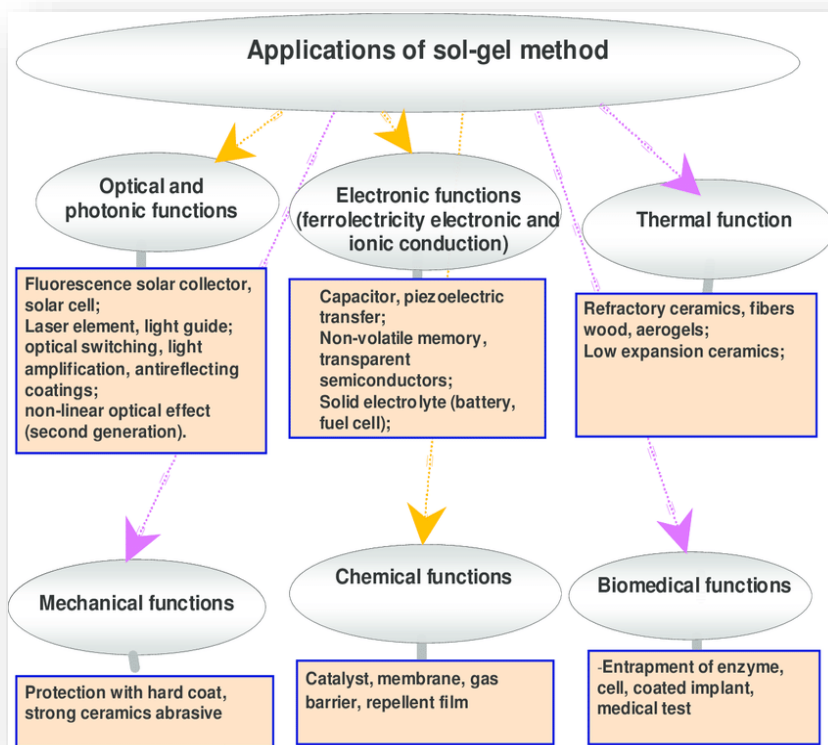


Figure II.9: Applications of sol gel method [17].

II.3. Preparation of pure ZnO powders doped with gallium «Ga» and «Bi»

The objective of our work is the production of pure zinc oxide powders doped with gallium and bismuth using the chemical sol-gel method. The following precursor chemicals were used in the preparation of ZnO powders:

- ✚ **Zinc acetate dehydrate ($C_4H_6O_4Zn \cdot 2H_2O$):** used as a starting material (which is shown in Figure II.10).
- ✚ **Citric acid monohydrate ($C_6H_8O_7 \cdot H_2O$):** acts as a catalyst for keep particles in suspension (which is shown in Figure II.10).
- ✚ **Ethylene glycol ($C_2H_6O_2$):** used as a solvent.
- ✚ **Gallium(III) nitrate hydrate ($Ga(NO_3)_3 \cdot H_2O$):** it is a source of gallium dopant «Ga».
- ✚ **Bismuth(III) nitrate ($Bi(NO_3)_3 \cdot 5H_2O$):** it is a source of bismuth dopant «Bi».



Figure II.10 : Zinc acetate dihydrate and Citric acid monohydrate.

The following table (II.1) represents some proprieties of the different precursors we used:

Table II.1: The physical and chemical properties of different chemicals used in this work.

| Chemical compound | Formula | Molarmass (g/mol) | Melting point(°C) | Appearance | Density (g/cm ³) |
|------------------------------|---------------------------|-------------------|-------------------|----------------------------|------------------------------|
| Zinc acetate dihydrate | $C_4H_8O_4Zn \cdot 2H_2O$ | 219.51 | 237 | White solid (all forms) | 1.84 |
| Citric acid monohydrate | $C_6H_8O_7 \cdot H_2O$ | 210.124 | 153 | white solid | 1.66 |
| Ethylene glycol | $C_2H_6O_2$ | 62.07 | -13 | Clear,colorless liquid | 1.28 |
| Bismuth(III) nitrate | $Bi(NO_3)_3 \cdot 5H_2O$ | 485.07 | 33 | colorless, white | 2.83 |
| Gallium(III) nitrate hydrate | $Ga_3NO_9 \cdot H_2O$ | 255.73 | 29.76 | Poudre cristalline blanche | 1.29 |

II.3.1. Preparation Steps

The preparation of nanopowders requires control of the experimental conditions, the important parameters are:

- ❖ The concentration of the chemical precursors.
- ❖ The temperature of the bath.
- ❖ The duration of the gel formation.
- ❖ The temperature of the calcination 500 °C.
- ❖ The duration of the calcination.

II.3.1.1. Cleaning glass

Cleaning glasses is a very important step to obtain high quality samples. The method used to clean is as follows:

- ❖ Wash with soap for at least 5 minutes.
- ❖ Rinse with distilled water.
- ❖ Clean with acetone for at least 5 minutes.
- ❖ Rinse with distilled water.
- ❖ Clean with ethanol for at least 5 minutes.
- ❖ Rinse with distilled water.
- ❖ Drying.

II.3.1.2. Pure ZnO nano-powders

The experiments were carried out by carrying in a silicone oil bath heated to a temperature, well fixed, two different glass beakers, in one of them a concentration $C_1=0.15\text{mol/l}$ of zinc acetate dissolved in ethylene glycol (AZ), and in the other a concentration $C_2=2.5\text{mol/l}$ of citric acid also dissolved in ethylene glycol (AC).

The homogeneity and the fixing is of the temperature, ensured by a thermo-contact, the homogeneity of the bath are ensured by means of a magnetic agitation.

After total dissolution of precursors and stabilization of temperature of oil bath both solutions were mixed, by adding gradually adding the solution of (citric acid + ethylene glycol) to solution of (zinc acetate + ethylene glycol) with a molar ratio ($C_1/C_2=0.06$), a transparent gel has been obtained which is maintained at the same temperature until total evaporation of the gaze and water.

The resulting solution was then agitated at 135°C for 6 hours to obtain a homogeneous and transparent solution. Finally the solution was Calcinated at 500°C for 6 hours.

II.3.2.2. Ga-doped ZnO nano-powders

Gallium oxide emerged as a material that travels between insulating behavior and half conductor, giving excellent and unique results as a semi-conductor material, characterized by its work in a very broad thermal field, having a very wide energy gap as it operates in the field of sub violet radiation, and its production cost is lower [18].

The same steps for the preparation of undoped ZnO (pure ZnO) were followed for the preparation of Ga-doped ZnO. We dissolved zinc acetate in ethylene glycol and adding a quantity of the gallium source: gallium nitrate (III) with an appropriate amount to obtain the desired concentrations (3 % Ga), the solution was charred at 500°C for 6 hours.

II.3.2.3. Bi-doped ZnO nano-powders

Bismuth oxide is an interesting material characterized by a significant band gap, high refractive index and dielectric permittivity, as well as marked photoconductivity and photoluminescence [19].

The same steps for the preparation of undoped ZnO (pure ZnO) were followed for the preparation of Bi-doped ZnO. We dissolved zinc acetate in ethylene glycol and adding a quantity of the gallium source: Bismuth nitrate (III) with an appropriate amount to obtain the desired concentrations (3 % Bi), the solution was charred at 500°C for 6 hours.

II.3.2.4. Ga+Bi co-doped ZnO nano-powders

The same steps for the preparation of undoped ZnO (pure ZnO) were followed for the preparation of Bi-doped ZnO. We dissolved zinc acetate in ethylene glycol and adding a quantity of the gallium source: Bismuth nitrate (III) and gallium nitrate (III) with an appropriate amount to obtain the desired concentrations (3 % Bi + 3 % Ga).

II.3.3. Calcination treatment

This is an operation which consists in transforming the gel into a powder by elimination. All traces of organic functions (acetic acid) and water vapours.

The thermal cycle at 500 °C , and the rate heat treatment is 5 °C/min.

Table II.2: Value of time of charred t_c per sample.

| Type of doped | ZnO pure | Ga -doped ZnO | Bi -doped ZnO | Ga_Bi co-doped ZnO |
|---------------|----------|---------------|---------------|--------------------|
| t_c (h) | 6 | 6 | 6 | 6 |

The figure below shows the pure and Ga , Bi doped ZnO powders with in this study.

**Figure II.11: The different samples prepared in our work.**

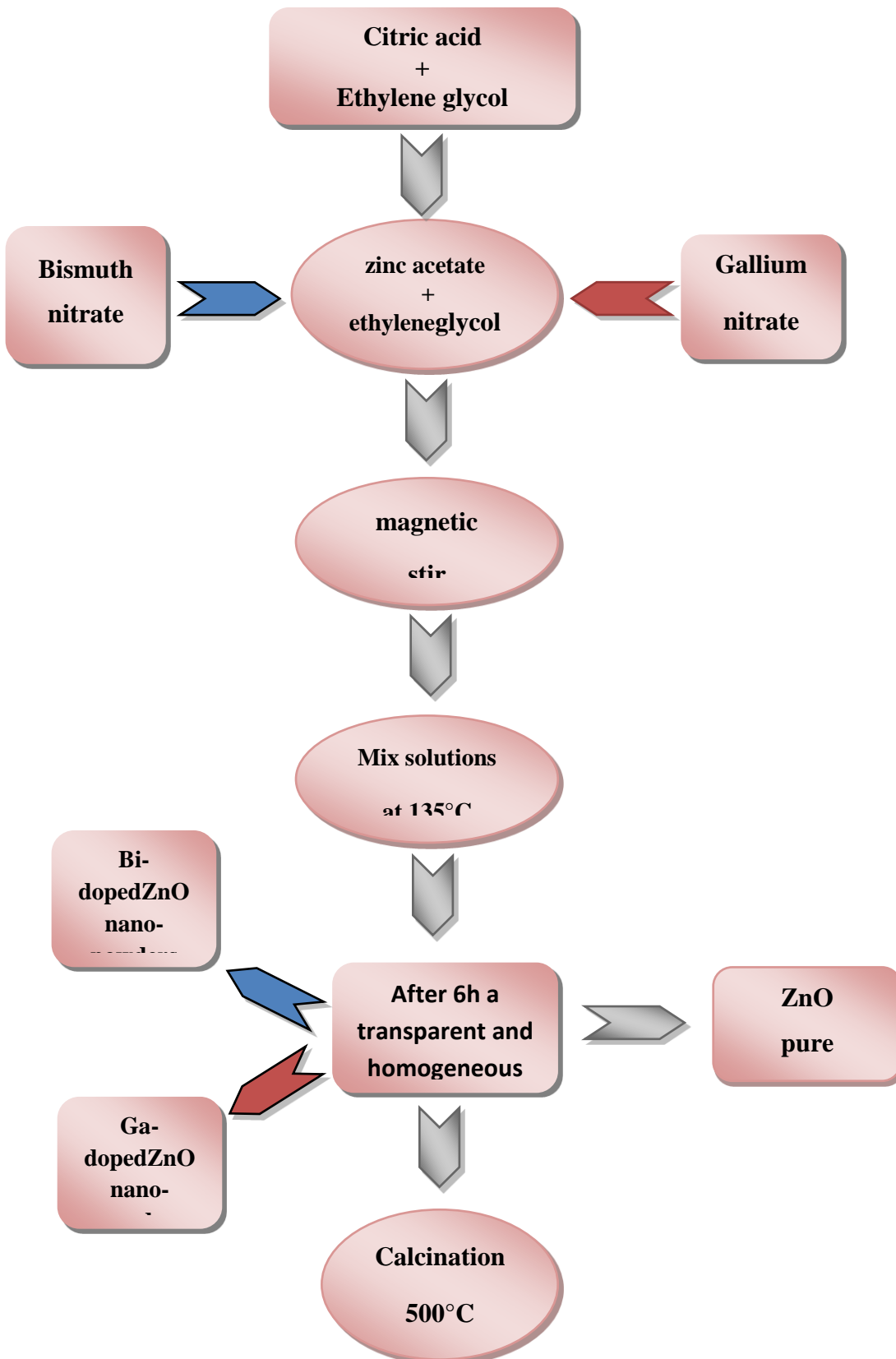


Figure II.12: The flow chart of major steps in the development of a ZnO powder pure and doped.

II.4. ZnO powder characterization techniques

Physical properties of ZnO powders obtained using different characterization techniques summarized in Table II.3. The composition of the crystals and the determination of the phase of the nanoparticles were studied using the X-ray diffraction scale (DRX). The spectrometer (FTIR) was used to assess the composition and structural quality of ZnO nanoparticles. The sample was analyzed for UV absorption and optical energy (e.g.) using UV spectrometry [20].

Table II.3: Overview of experimental techniques needed to study the morphology, structure and properties of ZnO nanoparticles [20].

| Technique | The collected information |
|-----------------------------------|---|
| X-ray diffraction (XRD) | degree of crystallinity, Orientation Crystal, Determination of the structure, Phase identification. |
| Fourier Infrared Transform (FTIR) | The quality of the composition, The analysis structural. |
| Spectroscopie UV-visible | Absorption, Transmission, Gap energy. |

II.4.1. X-ray diffraction

X-ray diffraction is a non-destructive structural analysis technique, it allows obtaining a lot of information about the sample: crystallization (or not), presence of parasitic phase(s), crystallographic parameters, orientation and grain size (inversely proportional to the mid-height width of the diffraction lines), and importance of the stresses due to the substrates (offset and shape of these lines) [8].

A monochromatic X-ray incident beam is focused on the sample to be characterized and interacts with the electronic cloud of these atoms. The principle of this technique therefore rests on the diffraction of monochromatic X-rays by the atomic planes of the crystals of the material studied (Figure II.13). Diffraction occurs when the Bragg relation is checked [21].

$$2 \cdot d_{hkl} \cdot \sin\theta = n \cdot \lambda \quad (\text{II.1})$$

Where :

- ✓ $d_{(hkl)}$ is Inter-channel distance.

- ✓ θ angle of incidence of X-rays on the surface of the studied material (angle of bragg).
- ✓ n is Order of refraction.
- ✓ λ is X-ray beam wavelength.

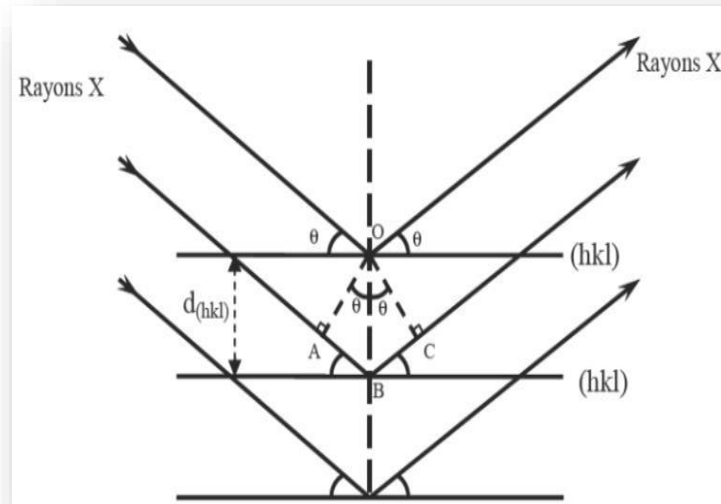


Figure II.13: The Principle of Bragg's Law[9].

II.4.1.1. Grain Size

Determine the size of the different sample gains for the first time from the spectrum of the diffraction. In order to ensure grain volume values we use shearer relation [21]:

$$D = \frac{0.9 \lambda}{\beta \cos \theta} \quad (\text{II.2})$$

Where:

- ✓ D is the size of the grains.
- ✓ β is the full width at half maximum of a diffraction line located at angle θ while λ is the X-Ray diffraction wavelength.

II.4.1.2. The interreticular distances and the cell parameters

The lattice parameter values for the Hexagonal systems can be calculated from the following quation using the (hkl) parameter sand the inter planar spacing d [22].

$$\frac{1}{d^2} = \frac{4}{3} \left(\frac{h^2 + hk + k^2}{a^2} \right) + \frac{l^2}{c^2} \quad (\text{II.3})$$

Where:

- ✓ a, c are the cell parameters .
- ✓ h, k, l are Miller's indices.

II.4.1.3. The lattice strain

The origin of micro strain ϵ is calculated using the relation [23]:

$$\epsilon = \frac{\beta \cos \theta}{4} \quad (\text{II.4})$$

II.4.1.4. The dislocation density

The dislocation density δ is the dislocation lines per unit of the crystal can also be evaluated from the crystallite size D using the formula:

$$\delta = \frac{1}{D^2} \quad (\text{II.5})$$

II.4.2. UV-Visible spectrophotometry

This technique rests on the knowledge of the distances between interference rings in the spectra of transmission in the visible and the near infra-red. One uses a recording spectrophotometer with double beams, of which its principle of operation is represented on figure (II.18).

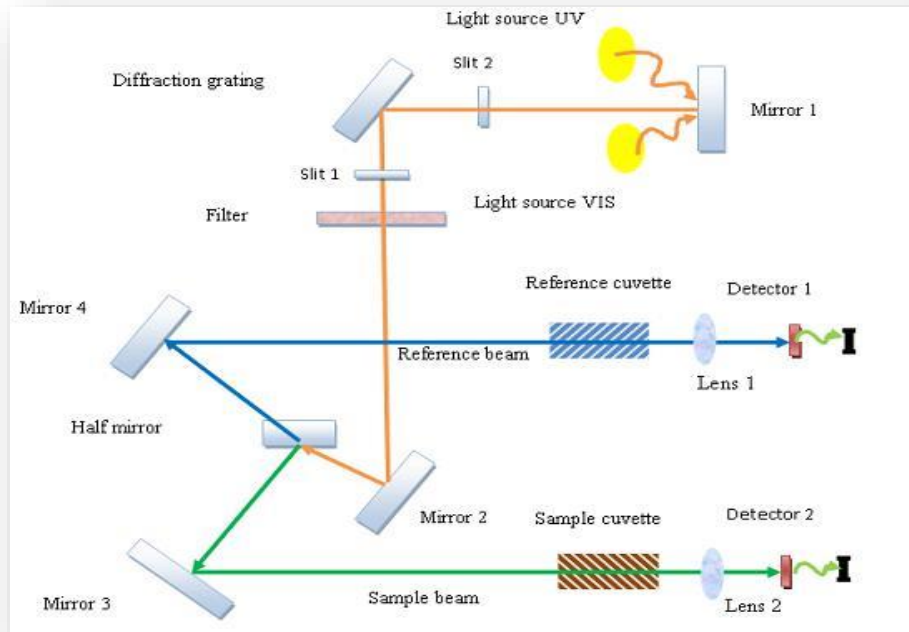


Figure II.14: The principle of operation of UV-visible [24].

The obtained spectra give the variation of transmittance expressed as a percentage (%) according to their wavelength .

Thanks to the interferences, one can determine the following parameters: Optical gap, Absorption coefficient and the refraction index which can be calculated using the following relation.

II.4.2.1. Absorption coefficient

In the spectral field where the light is absorbed, and by knowing the film's thickness, we can determine the absorption coefficient for each value of transmittance.

$$\alpha(cm^{-1}) = \frac{1}{d} l n \left(\frac{100}{T} \right) \quad (II.5)$$

T transmittance in (%) which corresponds to energy by the law of Beer-Lambert

$$T = \frac{I}{I_0} * 100 \quad (II.6)$$

Where:

$$\frac{I}{I_0} = \exp(-\alpha d) = \frac{T}{100} \quad (\text{II.7})$$

I_0 is the incidental light intensity, I the transmitted light intensity, α coefficient of absorption and d the thickness of the cell.

This approximate relation (II.5) is established, by neglecting the reflexions with all interfaces, air/cell [25].

II.4.2.2. Optical Gap E_g

In high energy, absorption results from electronic transitions between wide states of band to band. It is usually described by Tauc law [24]:

$$(\alpha h\nu) = A (h\nu - E_g)^m \quad (\text{II.8})$$

Where:

- ✓ $h\nu$ is the photon energy.
- ✓ E_g is optical gap and A are constants.
- ✓ m characterizes the optical type of transition and takes the values $\frac{1}{2}$ for allowed direct transitions or 2 for allowed indirect transitions[23].

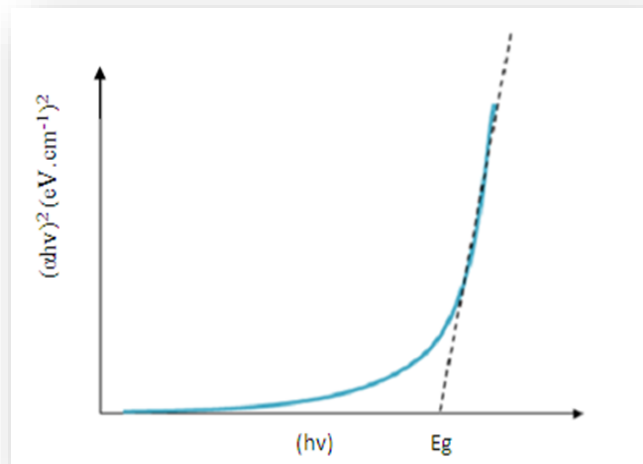


Figure II. 15: Determination of E_g [24].

II.4.2.3. Sample preparation

We measure a small amount of ZnO powder and dissolve it in the preferred solvent (hydrochloric acid 37%). After filling the cell with the solution (ZnO + hydrochloric acid 37%) and wipe it before placing it in a spectrometer.

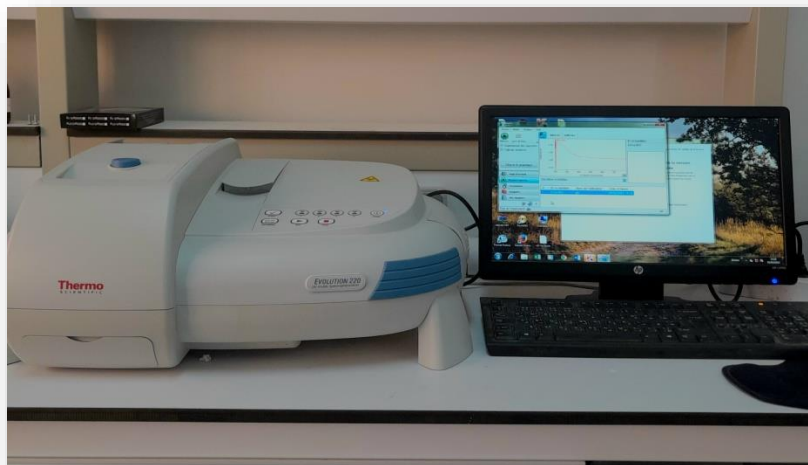


Figure II.16: EVOLUTION 220 spectrophotometer image.

II.4.3. Fourier Transform Infrared Spectroscopy (FTIR)

Fourier Transformed Infrared Spectroscopy (FTIR) is a non-destructive analysis technique based on the absorption of infrared radiation by the material being analyzed. It can detect the characteristic vibrations of the bonds and perform the analysis of the chemical functions present in the material. When the wavelength provided by the light beam is close to the molecule energy, the molecule will absorb the radiation and a decrease in the reflected or transmitted intensity will be recorded. Its range from 400 to 4000 cm^{-1} corresponds to the molecule vibration energy range [26].

The infrared beam is directed towards the Michelson interferometer which modulates each wavelength of the beam at a different frequency. In the latter, the incident light beam is separated in half by a separator. These two parts will reflect on mirrors, one of which is fixed and the other mobile. When the two beams recombine, destructive or constructive interference appears depending on the position of the moving mirror, as shown in (Figure II.15). The modulated beam is then reflected from the two mirrors to the sample, where absorptions occur. The beam then arrives on the detector to be transformed into an electrical signal [20].

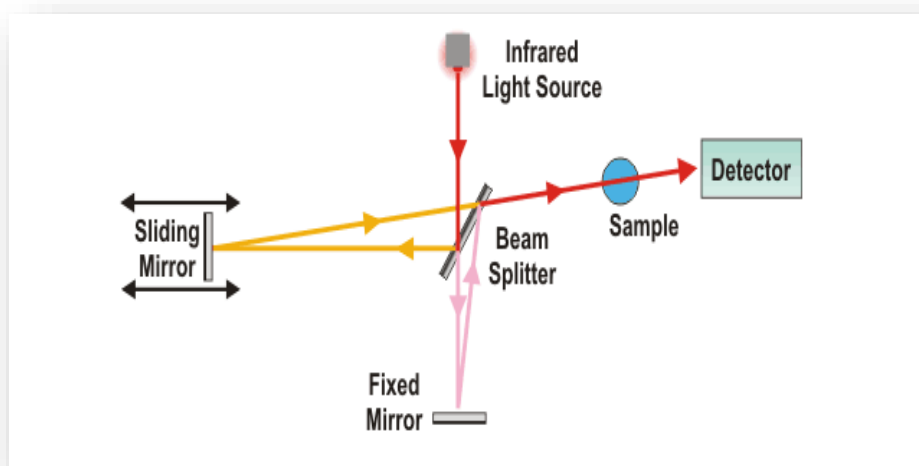


Figure II.17:The schematic representation of FTIR[27].

II.4.3.1. Sample preparation

Our IR spectra were recorded in solid phase in the region from 400 to 4000 cm^{-1} using a Thermo Scientific FTIR instrument (Nicolet 8400s)(see figure II.18).



Figure II.18: Thermo Scientific FTIR instrument (Nicolet 8400s).

The dried sample (1mg) is mixed with 300 mg KBr. The mixture is pressed in the form of a pellet using a uniaxial pressing, for 2 to 4 min.

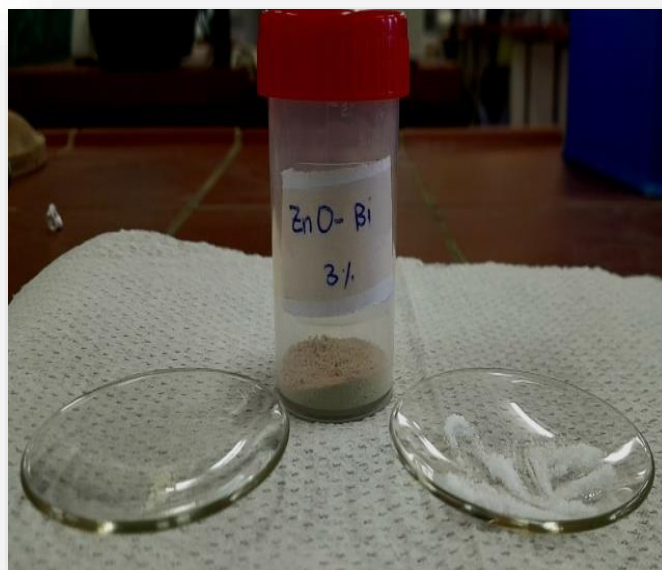


Figure II.19 : Preparation of sample for description IR .

References

- [1] Boumezoued A, (2020). Etude et préparation par Sol-Gel de nanomatériaux à base d'oxydes semiconducteurs et leurs applications ,These doctorah. Universite Larbi Ben Mhidi .Oum El Bouaghi.
- [2] Rawat R S, Dense plasma focus-from alternative fusion source to versatile high energy density plasma source for plasma nanotechnology. In Journal of Physics: Conference Series ,Vol. 591,2015, No. 1, p. 012021. IOP Publishing.
- [3] Danks AE, Hall, S R., Schnepf Z, The evolution of 'sol-gel' chemistry as a technique for materials synthesis. Mater. Horizons 2016, 3, 91–112.
- [4] Harouni S, Boulares N (2020). Elaboration et étude des propriétés physiques et chimiques de nanopoudres d'oxyde de zinc pour une application en photocatalyse hétérogène ,Doctoral dissertation, Université Frères Mentouri-Constantine 1.
- [5] Kaneva N V, Yordanov GG, Dushkin C D, Photocatalytic action of ZnO thin films prepared by the sol-gel method , React KinetCatal Lett, 2009, 98, 259- 263,
- [6] Mahcene F, Chari A, (2021). Synthèse par Sol-gel et caractérisation structurale et optique de nano poudres de ZnO pures et dopées en Aluminium (0.1, 0.5, 0.75, 1, 5, 7, 10, 15 et 20% at, Doctoral dissertation, Université Frères Mentouri-Constantine 1.
- [7] Guizard .C, Ecole d'été sol-gel, Tome 1. Centre National de la recherche Scientifique, Oleran 15-20,1991.
- [8] Boulassel A, Takkouk Z R, (2012). Synthèse par Coprécipitation et caractérisation des nanopoudres de l'oxyde de zinc. Etude de l'effet de dopage et de la température de calcination Doctoral dissertation. Université de jijel.
- [9] Amara N, (2020), Revêtements nano-composites nanofils de ZnO/nanoparticules destinés à l'éclairage à LEDs et à la photocatalyse .Doctoral dissertation, Université Clermont Auvergne . Sfax Tunis.
- [10] Bathat M, (1992), Microcavités optiques élaborées par voie sol-gel : applications aux ions terre rare d' Eu^{3+} et aux nanocristaux semiconducteurs de CdSe. These de Doctorat, Lyon.
- [11] Ponton A, Barboux C, Sanechez S, Rheology of titanium oxide based gels: determination of gelation time versus temperature , Colloids Surf. A, 2000, 162-177.

- [12] Grabsi I, Bouaicha F, Zaabat M . (2022). Elaboration et caractérisation des nanopoudres d'oxyde de fer par voie sol-gel. Mémoire de master , Université De Larbi Ben M'hidi Oum EL Bouaghi.
- [13] Owens G J, Singh RK, Foroutan F, Alqaysi M, Han C M, Mahapatra C, Knowles J C, Sol-gel based materials for biomedical applications. Progress in materials science, 2016, 77, 1-79.
- [14] Arab L, (2012), Elaboration par différentes méthodes et étude optique de poudres nanocristallines de ZnO pur et dopé par différents oxydes .Doctoral dissertation, Thèse de Doctorat, Université de Constantin..
- [15] Leautic A , Babonneau FJ, Structural Investigation of the hydrolysis condensation process of titanium alkoxides $Ti(OR)_4$ ($OR=Opr$, O) modified by acetylacetone. From the modified precursor to the colloids. Chemical Materials, 1989, 1 248.
- [16] Mehrotra RC, Synthesis and reactions of metal alkoxides, J. Non-Cryst. Solids 1988, 100, 15 .
- [17] Dimitriev Y, Ivanov Y, Iordanova R, History of sol-gel science and technology. Journal of the University of Chemical technology and Metallurgy, 2008, 43(2), 181-192.
- [18] كيجول ن , محاكاة تأثير وصلة شوتكي لثنائية من اكسيد الجاليوم , مذكرة ماستر , جامعة محمد خيضر بسكرة.
- [19] Leontie L, Caraman M, Alexe M , Harnagea C, Structural and optical characteristics of bismuth oxide thin films. Surface Science, 2002, 507, 480-485.
- [20] Geurram A, (2022), Synthèse verte et caractérisation des nanoparticules de ZnO à l'aide d'extrait des feuilles de Phoenix dactylifera L et leur applications , Doctoral dissertation, Faculté des Sciences et de la technologie.
- [21] Bouaichi F, (2010). Dopage et caractérisation des couches minces d'oxyde de Zinc déposées par spray pyrolyse Ultrasonique , Doctoral dissertation. University Mohamed Khider of Biskra.
- [22] Aldrin A ,(2004), Preparation and characterization of certain II-VI, I-III-VI₂ semiconductor thin films and transparent conducting oxides, Doctorat Thesis, Cochin University of Science and Technology, Kerala, India.
- [23] Nezzal H, Rajouhe N E H, (2022), Elaboration of pure and Bi-doped ZnO nano-powders with the sol-gel method. Memory of master .University Mohamed Khider of Biskra.
- [24] Dahnoun M, (2020), Preparation and Characterization of Titanium dioxide and Zinc oxide thin films via Sol-Gel (spin coating) technique for optoelectronic applications, Doctorat Thesis. University Mohamed Khider of Biskra
- [25] Kasap S, Capper P, Springer Handbook of Electronic and Photonic Materials , Springer Science and Business Media , 2006.

- [26] Bozetine H, (2017), Synthèse des nanostructures de ZnO par la méthode hydrothermale et leurs applications ,Doctoral dissertation, Université Mouloud Mammeri .
- [27] <https://www.tribonet.org/wiki/fourier-transform-infrared-spectroscopy>.

Chapter III

Results and discussions

In this chapter we present the results obtained for zinc oxide (ZnO) nanopowders pure and doped with gallium and bismuth developed by the chemical soil-gel method..

The results of this study are obtained by various characterization methods: X-ray diffraction (DRX) for the study of structural properties. The UV-Vis spectrophotometer to determine the optical properties of pure ZnO and doped with gallium and bismuth. The infrared IR spectroscopy for the study of chemical properties.

III.1 Results and discussions

III.1.1. Structural study

X-ray diffraction (XRD) was performed using the Mini-Flex (Rigaku) wavelength diffraction measure = 1.5405 \AA , between 20 to 80 degrees (2θ). XRD patterns of pure and doped ZnO powders were reported with different doping (3%Ga and 3% Bi) respectively. (Figures III.1-III.3)

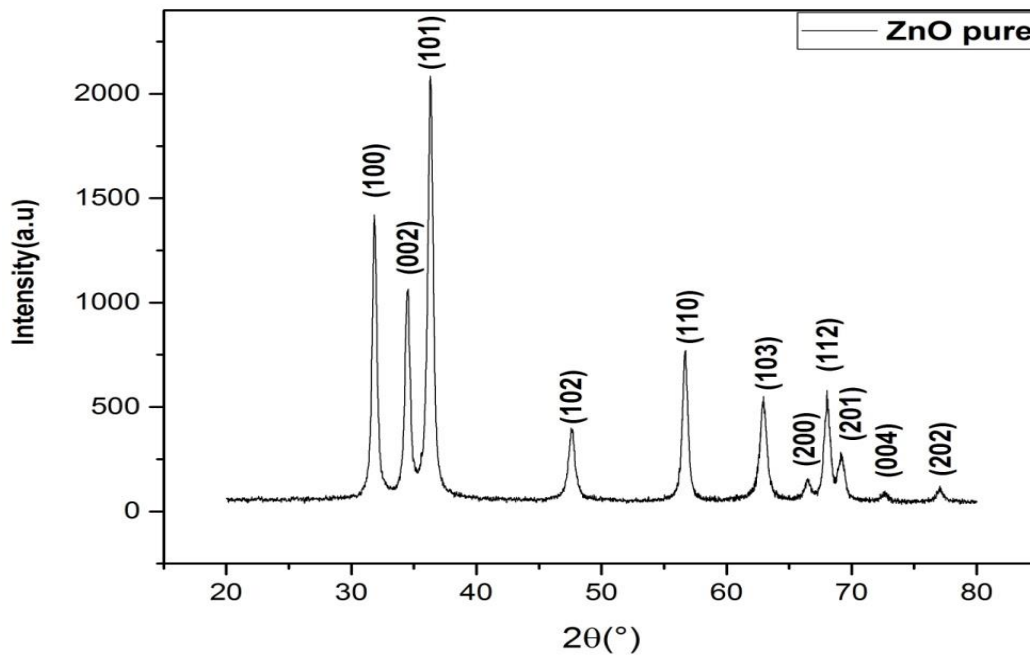


Figure III.1: XRD patterns of ZnO pure powders.

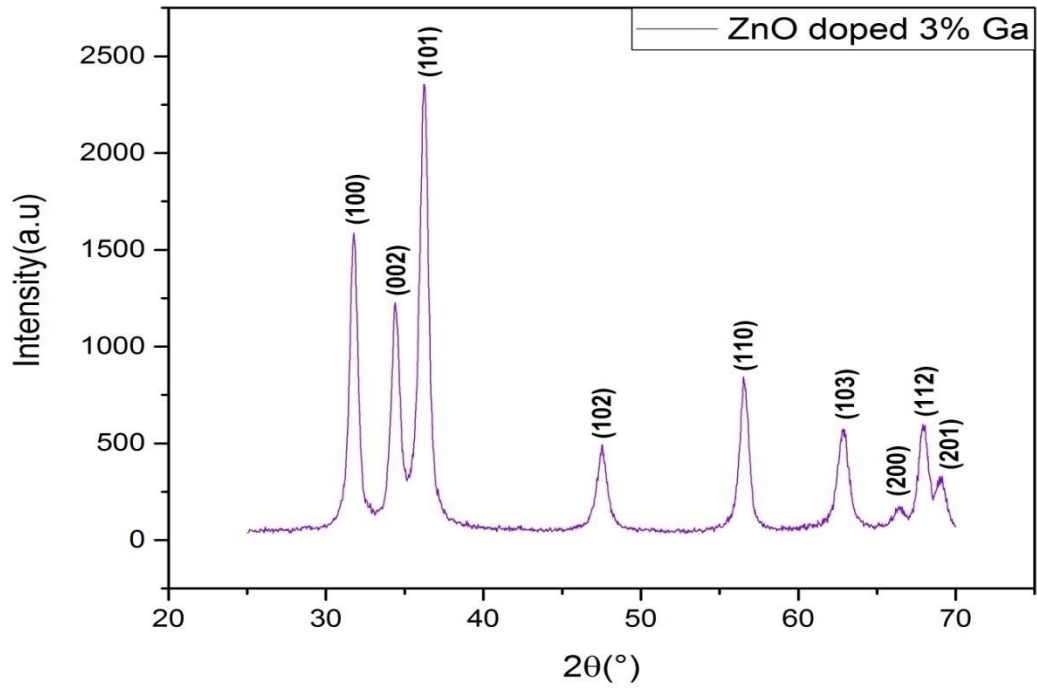


Figure III.2: XRD pattern of ZnO doped 3% Ga.

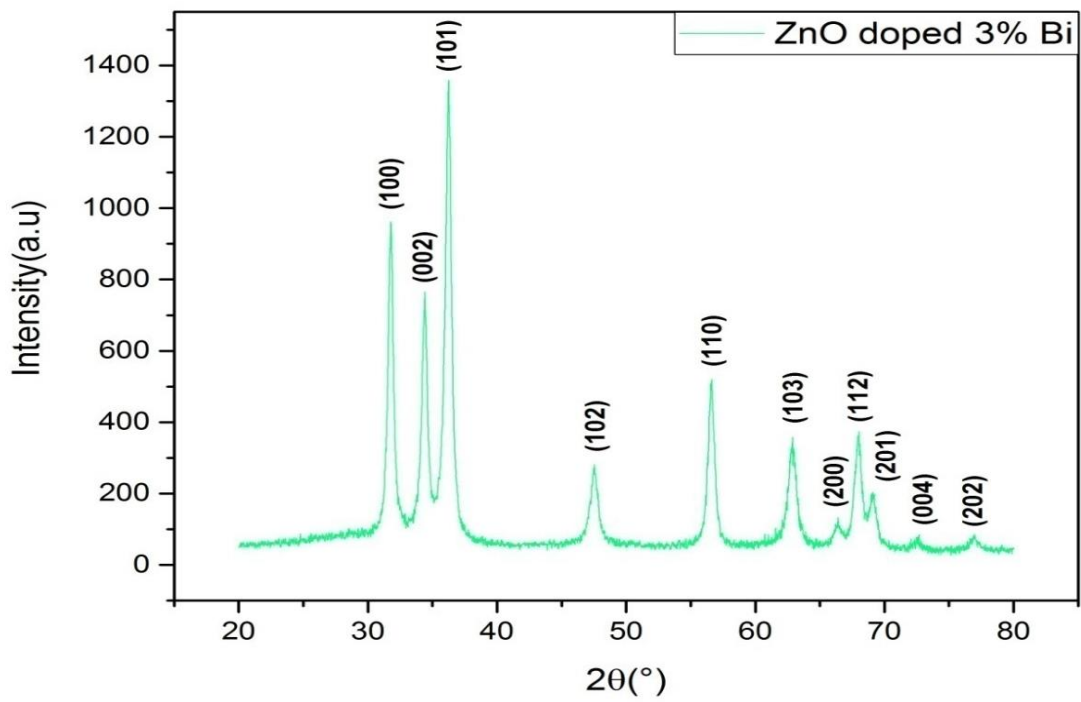


Figure III.3: XRD pattern of ZnO doped 3% Bi.

Figures (III.1, 2, and 3) show the X-ray diffractions patterns of pure ZnO and ZnO doped with 3% of Ga and 3% of Bi respectively. It's clear that no new peak associated to Ga or Bi is recorded, so we can say that the elaboration powders are solid solutions.

DRX spectrums for pure ZnO and doped 3% Ga, and doped 3% Bi show a high level of crystallization in the following directions (100), (002) and (101), i.e. the structure has preferred growth directions.

III.1.1.1. Crystallite size, Lattice strain and Dislocation density variation

The crystallite size was calculated using the Scherer formula (II.2) and formulas (II.4 and 5) to calculate lattice strain ϵ (%) and dislocation density δ (nm^{-2}) respectively.

Table III.1: A summary table of the structural parameters of dopage types.

| | (hkl) | 2θ ($^{\circ}$) | Crystallite size D (nm) | Lattice strain ϵ (%) | Dislocation density δ (nm^{-2}) |
|---------------------|-------|--------------------------|----------------------------|----------------------------------|--|
| ZnO pure | 101 | 36.32 | 16.952 | 0.204 | 0.00347 |
| ZnO doped Ga | 101 | 36.22 | 11.556 | 0.299 | 0.00748 |
| ZnO doped Bi | 101 | 36.23 | 14.762 | 0.234 | 0.00458 |

The decrease in D is due to the difference in the ion diameters of Zn^{+2} and Ga^{+3} , where this later takes alternate locations of Zn^{+2} ion, which reduce the core cell constants and therefore decrease the crystallite size D, this result was previously found by A. Khorsand Zak et al. [1].

Although the ion diameter of the Bi^{+3} ions is larger than that of Zn^{+2} ions, we have noticed a decrease in crystallite size, this remark is due to the fact that Bi plays a stimulating role that disrupts the crystal structure and provides structural defects. These defects can hinder the

growth of crystals and enhance the formation of smaller crystals, resulting in lower crystal size. Approximately the same conclusion was reported by Kumar et al. [2].

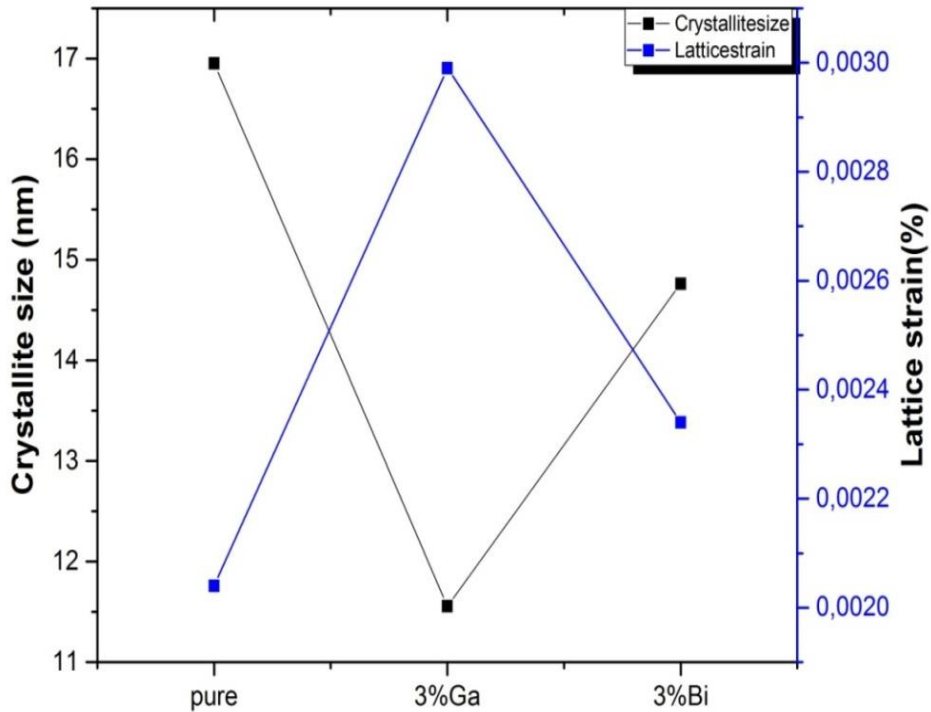


Figure III.4: Crystallite size and the strain as functions of doping types.

Figure (III.4) shows a reverse behavior of ϵ lattice strain and crystallite size for all nanopowders. The crystallite sizes of doped ZnO nanopowders are lower than crystallite sizes recorded for pure ZnO nanopowder. The lowest crystallite size is the one of Ga-doped ZnO nanopowder. This result has been explained in the precedent paragraph. On the other side, the deformation changes as grain volume changes. This is the result of the addition of both Ga or Bi atoms in the ZnO matrix (pressure or extension).

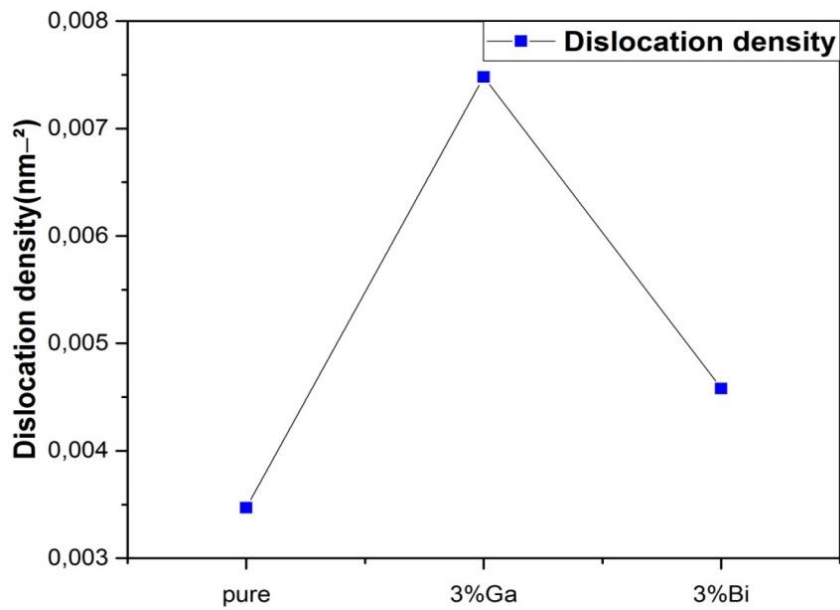


Figure III.5: The dislocation density as functions of doping type.

We note a tender relation between the intensity of dislocation δ and the network stress ϵ , as well as the intensity of dislocation increases the lattice strain increases, however, an opposite behavior is recorded for the crystallite size. Moreover, dislocations naturally become longer as dislocation lines extend to avoid micro-structural barriers that enhanced by the decrease of crystallite size [3].

III.1.1.2. Lattice parameters

The lattice parameters a and c are calculated using peaks (100) and (002) for pure ZnO, doped-ZnO with 3% Ga and ZnO doped with 3% Bi.

Table III.2: Lattice parameters of dopage types.

| | a (Å) | c (Å) |
|------------------------|-------|-------|
| ZnO pure | 3.22 | 5.27 |
| ZnO doped 3% Ga | 2.86 | 4.67 |
| ZnO doped 3% Bi | 3.34 | 5.54 |

The first view of the Table shows that: increased of parameters "a" and "c" of Bi and decreased parameter of Ga , this difference is expected and is based on the difference in the values of the ionic radius of the Bi^{+3} and Ga^{+3} , Zn^{+2} ions.

III.1.2. Optical study

Shapes (III.7 to III.10) show transmission spectrums for pure ZnO and doped , we obtained the optical band gap E_g of pure and doped ZnO by extrapolating the linear portion of the plot $(\alpha h\nu)^2$ on function $(h\nu)$.

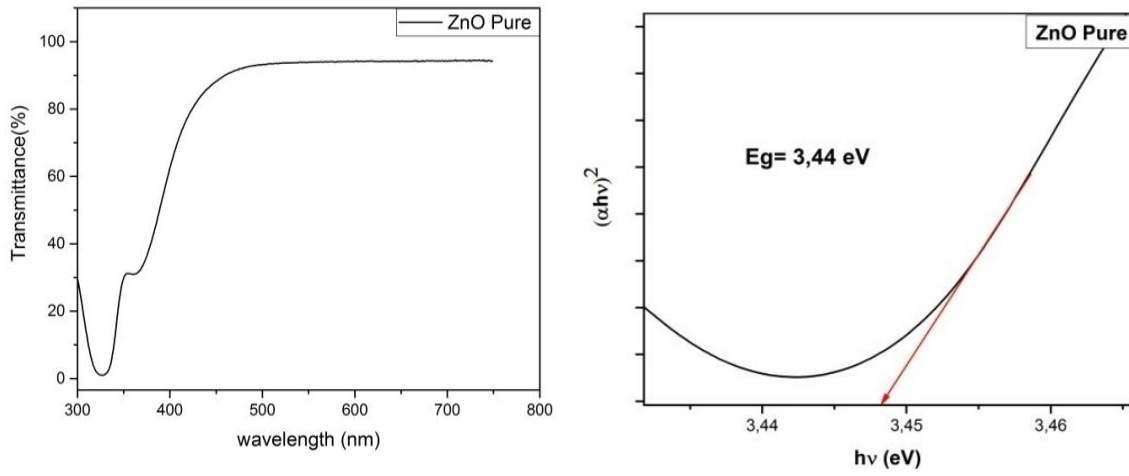


Figure III.6: The transmittance spectra of ZnO pure and plots of $(\alpha hv)^2$ on function $h\nu$ of ZnO pure.

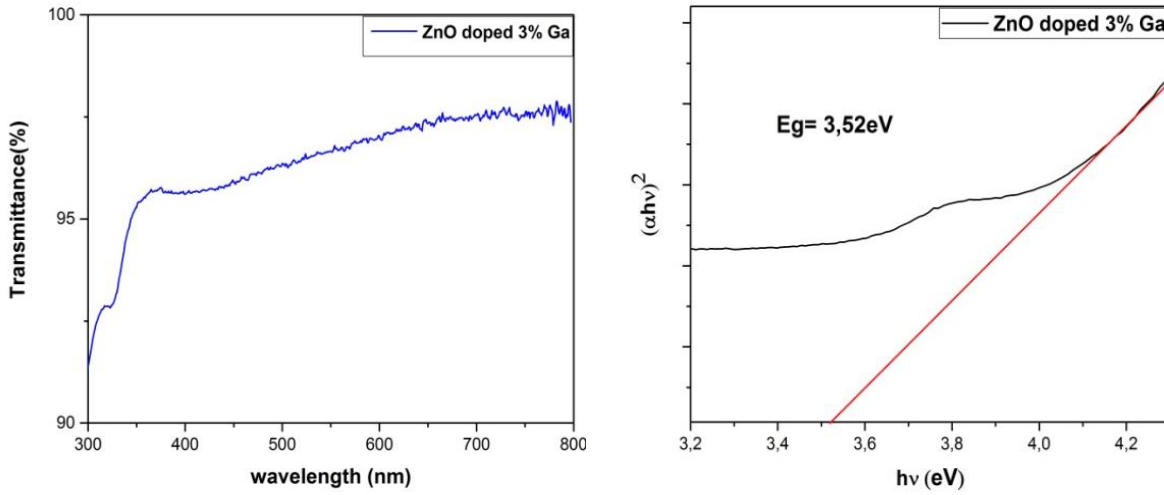


Figure III.7: The transmittance spectra of 3% Ga doped ZnO and plots of $(\alpha hv)^2$ on function $h\nu$ of 3% Ga doped ZnO.

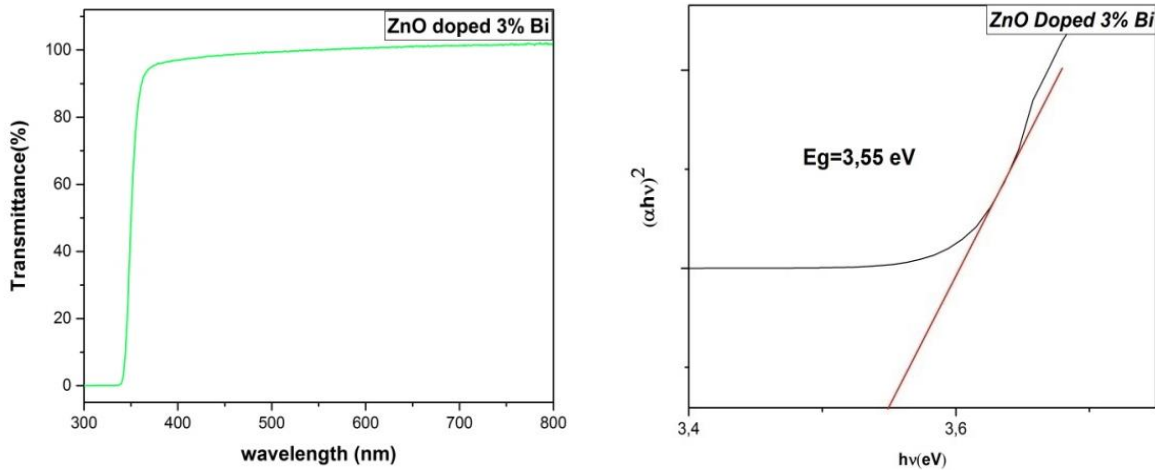


Figure III.8: The transmittance spectra of 3% Bi doped ZnO and plots of $(\alpha hv)^2$ on function hv of 3% Bi doped ZnO.

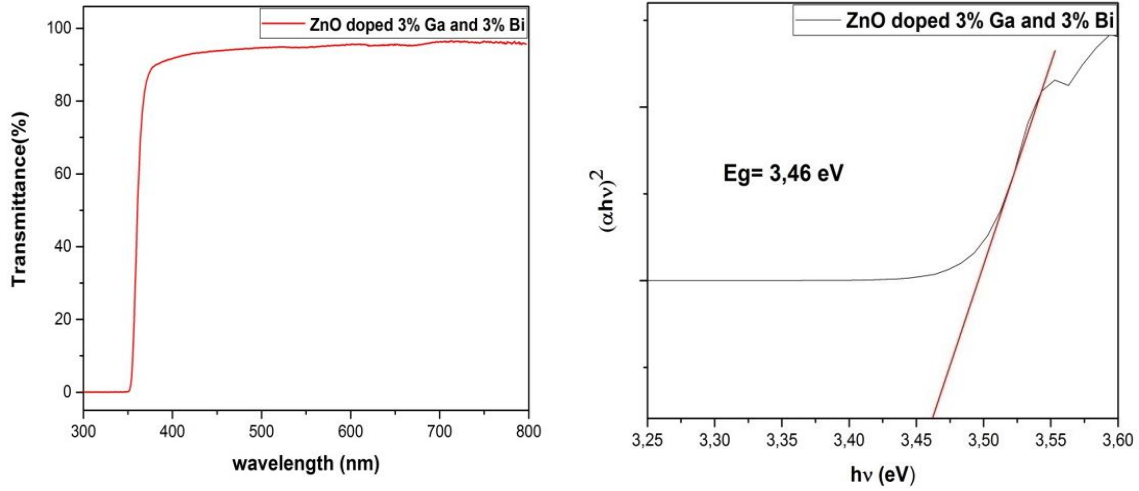


Figure III.9: The transmittance spectra of 3% Ga+3%Bi doped ZnO and Plots of $(\alpha hv)^2$ on function hv of 3% Ga+3%Bi doped ZnO.

Figures (III.6 to III.9) show transmission spectrums and schemes $(\alpha hv)^2$ on function hv for pure and doped-ZnO by Bi and Ga. Pure and doped zinc oxide transmittance spectrums show that the transmittance margin is between 322.32 nm and 348.10 nm. A large number of factors can affect the optical gap energy including: grain size, grid standard and bond length, film crystallization and crystal defects due to impurities and/or other defects, grid strain and stress [4, 5].

Table III.3: Optical band gap values of undoped and doped ZnO.

| Products | ZnO pure | ZnO doped 3% Ga | ZnO doped 3% Bi | ZnO doped 3% Ga+3% Bi |
|----------------------|----------|-----------------|-----------------|-----------------------|
| Band gap (eV) | 3.44 | 3.52 | 3.55 | 3.46 |

Compared to the undoped ZnO sample, all the doped samples show an increase in E_g (table III.3), with Bi doped ZnO displaying the greater E_g (3.55 eV) and the 3% Ga+3%Bi co-doped sample at $E_g = 3.46$ eV. This widening range gap phenomenon has been reported in many literature for ZnO stimulants and can be explained by the Burstein-Moss effect.

Burstein Moss effect is observed when adding impurities to equip vectors. New energy levels of added impurities will be added so that the latter overlap and are very close to band

valence (BV) or band conduction (BC). Here the energy needed for electrons to move from one level to another will increase [4].

In the absence of a strong correlation between E_g and B_v , the observed decrease of E_g with TM doping could be a consequence mainly of Ga and/or Bi incorporation (substitutional and/or interstitial) into the ZnO wurzite structure along with charge-compensating oxygen vacancies and introduction of other possible defects [6].

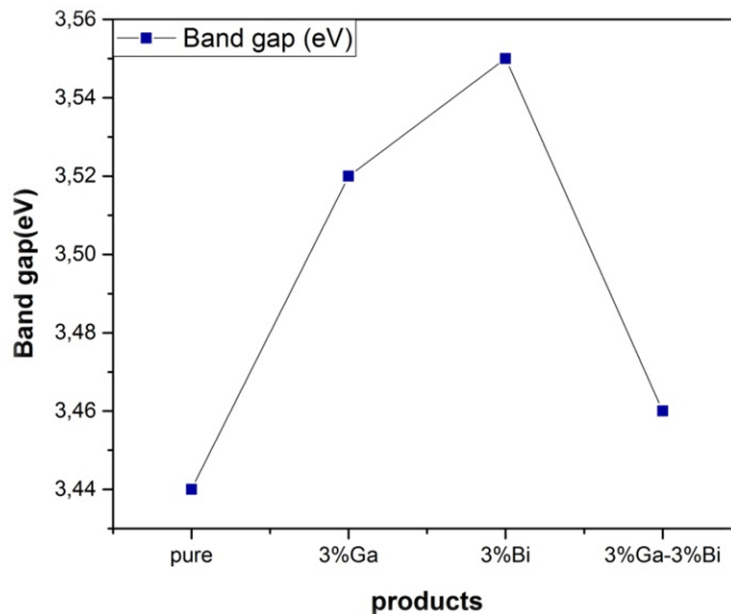


Figure III.10 Variation of the band gap with types of the doping.

III.1.3. Chemical study

Figure (III.11) shows the FT-IR spectrum of pure and doped ZnO samples in the range $4000\text{--}400\text{ cm}^{-1}$, a more pronounced peak was recorded at wave number 432.025 cm^{-1} on all spectrums, which returns to the **Zn-O** band, showing this peak in all doping types, especially for Bi, to which we can add greater transmission compared to other types. The second distinction is the double band **C=O** where clear selection 2 peaks (asymmetric and symmetric) was observed with respect to the extended vibration model, which was observed at specific wavelengths (equal to 1397.83 cm^{-1} and 1590.17 cm^{-1} respectively). The loyal peak returns to the CO_2 bond which can be formed through atmospheric air at 2347.207 cm^{-1} . Peaks located at 2933.69 cm^{-1} and 3303 cm^{-1} , are due to **C-H** and **O-H** bonds, respectively, which appear due to experimental conditions (environmental pollution).

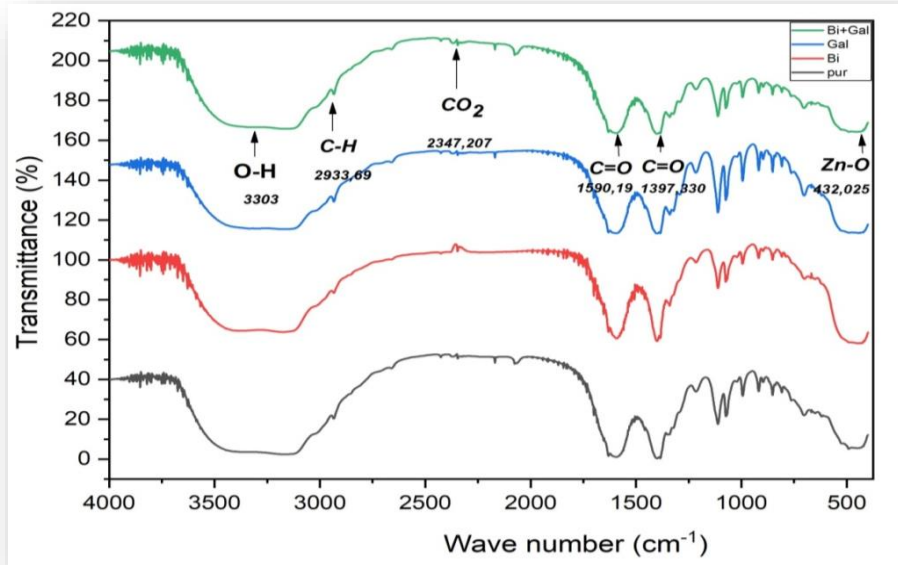


Figure III.11: FTIR spectra of ZnOpur and 3%Ga-doped ZnO and 3%Bi-doped ZnO and 3%(Ga+Bi) -doped ZnO.

References

- [1] Khorsand Z A, Abd Aziz N S, Hashim A M, Kordi F, Ceramic international. 42, 2016,13605-13611.
- [2] Ratheesh K, P M, Kartha C S, Vijayakumar K P, Doping of spray-pyrolyzed ZnO thin films through direct diffusion of indium: Structural optical and electrical studies, Journal of Applied Physics, 2005. 98(2), 023509.
- [3] Yahia A, (2020), Optimization of Indium Oxide Thin Films Properties Prepared by sol gel Spin Coating Process for Optoelectronic Applications, Doctorat thesis, University Mohamed Khider of Biskra.
- [4] Beltrán J J, Osorio J A, Barrero C A, Hanna C B , Punnoose A, Magnetic properties of Fe doped, Co doped, and Fe+ Co co-doped ZnO. Journal of Applied Physics,2013, 113(17), 17C308.
- [5] Mahdhi H, Ayadi Z B, Alaya S, Gauffier JL, Djessas K, Superlattice. Microst. 72 T.Ivanova et al. / Journal of Molecular Structure. 1206 (2020) 127773 10 (2014) 60-71.
- [6] Zhao J L, Sun X W, Ryu H, Moon Y B, Thermally stable transparent conducting and highly infrared reflective Ga-doped ZnO thin films by metal organic chemical vapor deposition. Optical materials,2011, 33(6), 768-772.

General conclusion

General conclusion

The work carried out in this memory consists in the synthesis of nanopowders of pure zinc oxide and doped with Gallium (Ga) and Bismuth (Bi) with concentrations of 3%, by the sol-gel process, this method is inexpensive and easy to implement.

We characterized the pure and Ga, Bi doped zinc oxide by different methods: X-ray diffraction (DRX) for structural study, UV-Visible spectroscopy for studying optical properties, Fourier transformation infrared spectroscopy (FTIR) for the study of chemical properties.

- XRD results confirm the ZnO synthesized powders crystallize in a hexagonal würtzite structure and it show difference of both the size of the grain, the intensity of the dislocation, and the strain lattice.
- The results of the UV-Visible analysis also allowed us to know the value of the range gap so that it increases according to the type of dopant.
- From infrared IR spectroscopy, we found distinctive ZnO semiconductor peaks (Zn-O band).

This research can be further improved and strengthened by many other studies.

Abstract

Abstract

In this work, pure ZnO and Bi-doped ZnO and Ga-doped ZnO and (Ga+Bi)-doped ZnO nanopowders with concentrations 3% , have been successfully synthesized with a soft chemistry method: the sol-gel. This method produces samples with high purity, homogeneity, and a structure of easy control. The powders have been characterized using the following techniques: X-ray diffraction (XRD), UV-visible spectroscopy (UV-Vis), and Fourier transform infrared (FTIR) spectroscopy.

The XRD results confirm that all the samples exhibit a polycrystalline hexagonal wurtzite structure of the ZnO. The results of UV analysis showed a increase in the values of the band gap energy (E_g). In addition, Fourier transforms infrared (FTIR) spectroscopy showed the presence of a zinc oxide-specific bond in the samples.

Keywords: zinc oxide, Bismuth, Gallium, nanopowder, sol-gel, XRD, UV-Vis, FTIR

ملخص

في هذا العمل، تم تصنيع مسحوق أكسيد الزنك النقي ومسحوق أكسيد الزنك المطعم بالبزميت وأكسيد الزنك المطعم بالجاليوم وأكسيد الزنك المطعم بالبزميت والجاليوم بتركيزات 3% بنجاح باستخدام طريقة الكيمياء اللينة: الصول-جل، تنتج هذه الطريقة عينات عالية النقاء والتجانس وهيكل سهل التحكم به . تم تحليل المساحيق باستخدام التقنيات التالية: حيود الأشعة السينية (XRD) ، والتحليل الطيفي المرئي بالأشعة فوق البنفسجية (UV-Vis) ، والتحليل الطيفي لتحويل الأشعة تحت الحمراء (FTIR) .

تؤكد نتائج XRD أن جميع العينات تظهر بنية سداسية الوترتيت متعددة البلورات ZnO، أظهرت نتائج تحليل الأشعة فوق البنفسجية زيادة في قيم طاقة فجوة النطاق (E_g). بالإضافة إلى ذلك، أظهر التحليل الطيفي للأشعة تحت الحمراء (FTIR) وجود رابطة خاصة بأكسيد الزنك في جميع العينات.

الكلمات المفتاحية: أكسيد الزنك، بزميت، جاليوم، مساحيق نانولورية، صول-جل، الخصائص الهيكلية والبصرية.